JOURNAL OF NEUROPHYSIOLOGY
Vol. 48, No. 4, October 1982. *Printed in U.S.A.*

Slow Active Potentials and Bursting Motor Patterns in Pyloric Network of the Lobster, *Panulirus interruptus*

DAVID F. RUSSELL AND DANIEL K. HARTLINE

Békésy Laboratory of Neurobiology, University of Hawaii, Honolulu, Hawaii 96822; and Department of Biology, University of California, La Jolla, California 92037

SUMMARY AND CONCLUSIONS

1. Neurons in the central pattern generator for the "pyloric" motor rhythm of the lobster stomatogastric ganglion were investigated for the possible involvement of regenerative membrane properties in their membrane-potential oscillations and bursting output patterns.

2. Evidence was found that each class of pyloric-system neurons can possess a capability for generating prolonged regenerative depolarizations by a voltage-dependent membrane mechanism. Such responses have been termed plateau potentials.

3. Several tests were applied to determine whether a given cell possessed a plateau capability. First among these was the ability to trigger all-or-none bursts of nerve impulses by brief depolarizing current pulses and to terminate bursts in an all-or-none fashion with brief hyperpolarizing current pulses. Tests were made under conditions of a high level of activity in the pyloric generator, often in conjunction with the use of hyperpolarizing offsets to the cell under test to suppress ongoing bursting.

4. For each class, the network of synaptic interconnections among the pyloric-system neurons was shown to not be the cause of the regenerative responses observed.

5. Plateau potentials are viewed as a driving force for axon spiking during bursts and as interacting with the synaptic network in the formation of the pyloric motor pattern.

INTRODUCTION

The intracellular activity of a neuron participating in rhythmic bursting can be described in terms of several phases, without regard to mechanisms. A prolonged depolarization usually underlies the impulse burst. The prolonged depolarization terminates in a repolarization phase. The interburst interval then follows.

Considering only the prolonged depolarization phase, one type of mechanism that has been demonstrated in several bursting systems is that of membrane negative resistance. Voltage-dependent inward-current mechanisms with slow kinetics can give rise to prolonged regenerative "plateau potentials," resembling in form and mechanism the plateau phase of the action potential of vertebrate cardiac muscle. In principle, the membrane potential is quasi-stable at two voltages on the voltage-current relation, where net membrane current is zero: a "rest" level and a depolarized "plateau" level. Transitions both to the plateau level and back to the rest level are threshold processes, voltage dependent and regenerative (1, 11, 22, 28, 33, 46, 48, 54).

This study concerns the pyloric rhythm of lobsters, governing the operation of valves and filters in the pylorus of the stomach during food digestion (19, 25, 26). The rhythm is active in isolated preparations of the foregut nervous system, being produced under these conditions by a central pattern generator composed mainly of 14 neurons in the stomatogastric ganglion (STG). The STG is advantageous for studying pattern generation due to its small number of neurons (about 30), their individual reidentifiability, and the restricted numbers of synaptic interconnections, as detailed elsewhere (17, 19, 25, 27). In essence, the pyloric rhythm has been

0022-3077/82/0000-0000$01.25

thought to be driven by a group of endogenously repetitive bursting neurons (the pyloric dilator-anterior burster (PD-AB) "driver" cells), which periodically inhibit the other ("pyloric follower") neurons. Of special interest here is what causes the pyloric follower neurons to depolarize and fire impulses.

We have analyzed the electrical properties of prolonged depolarizations underlying bursts in the pyloric follower neurons and conclude that they behave in many ways, both spontaneously and in response to experimental tests, like slow regenerative potentials in other excitable systems (1, 11, 13, 20, 23, 33, 34, 43, 45, 46, 48, 52, 53). The indirect tests and criteria that we have applied are based on familiar concepts of voltage dependency, threshold, regenerativeness, and all-or-none character, which can be interpreted in terms of a negative-resistance characteristic due to endogenous membrane mechanisms of a cell. We focus on the positive-going voltage excursion forming the burst onset and the duration of the prolonged depolarization underlying the burst, because at these phases in the rhythm cycle synaptic interactions in the pyloric generator are minimal and could be excluded as a basis for the observed behavior. We show that all the pyloric follower neurons can generate slow regenerative depolarizations, and where possible we also show that the regenerative characteristic turns on and off over the normal range of membrane potential. It is likely that regenerative plateau potentials are a major driving force for the impulse bursts in all the pyloric follower neurons (40, 41).

METHODS

Preparation and instrumentation

In vitro preparations from California spiny lobsters, *Panulirus interruptus*, were used. The foregut was removed and its nervous system dissected away, transferred to a Sylgard-lined petri dish filled with standard aerated saline (42), and arranged as in Fig. 1. After desheathing the STG and applying extracellular "pin" electrodes to motor nerves and central connectives, STG neurons were impaled for intracellular analysis. Experiments were at room temperature (18–22°C). Preparation condition remained usable (often slowly declining) for usually about 12 h.

Data were from a series of over 90 experiments, designated *G1–G90*. Results reported in this article were mainly from "combined preparations" (Fig. 1*A*) in which the paired commissural ganglia, the esophageal ganglion, and the STG were dissected with their connecting nerves intact (Son's Ion's, Stn; Refs. 31, 37). Spontaneous input from the commissural ganglia acts to greatly enhance bursting activity in the STG generators (36, 37, 49). Data on PD-AB cells (Fig. 4) were from three experiments with the commissural ganglia removed so that PD-AB activity was moderate (39; the esophageal ganglion was still connected to STG).

Impaled STG neurons were identified by the peripheral distribution of their axons, in conjunction with synaptic connections, phase in a rhythm, etc. (18, 19, 26, 27). A cell of primary interest was impaled usually with separate "voltage" and "current" micropipettes (filled with 3 M KCl, sometimes 4 M K acetate, 30–60 M), although double-barrel electrodes were occasionally used, as noted in the legends.

Figure 1*A* also indicates the use of combinations of Vaseline pools, applied with a syringe, to bathe nerves and ganglia in various solutions (37, 39). With pool 1, the commissural and esophageal ganglia could be bathed in "low-Ca^{2+}" saline (either 0.1 × Ca^{2+}-6 × Mg^{2+} or 0 Ca^{2+}-2 × Mg^{2+}; see Ref. 42); the commissural ganglia were desheathed in that case to improve diffusion. Pools 2, 3, and 4 were used to reversibly block impulse conduction in a nerve by bathing it in a pool of isotonic sucrose solution (37, 39; pool 2 was sometimes made as separate pools around each Ion). To counteract evaporation, solutions in pools were renewed periodically or a continuous flow system was used.

Oscilloscope sweeps and intracellular stimuli were routinely synchronized to the pyloric rhythm, using a trigger and a ramp generator. The start of a burst in PD cells (recorded with a pyloric dilator nerve or intracellularly) was taken as a constant reference point in the pyloric rhythm, since the PDs are part of the driver group. Other instrumentation included 12 channels of nerve preamplifiers, a 14-channel FM tape recorder (DC-2,500 Hz) for data collection, W-P Instruments amplifiers (M4-A, 701) with constant-current generators, a compensation circuit to null the resistive coupling between microelectrodes, a virtual-ground operational amplifier current monitor in the bath ground return, and a rectilinear pen recorder to monitor the absolute membrane potential, often verified by disimpalement.

Nomenclature

The naming system for neurons follows that of Maynard and Dando (26) except that "PY" neurons have been subdivided into PL and PE subtypes (18), and the "pyloric P-interneurons" have been included (36–38) (Table 1). To simplify figures, many extracellular traces are identified by

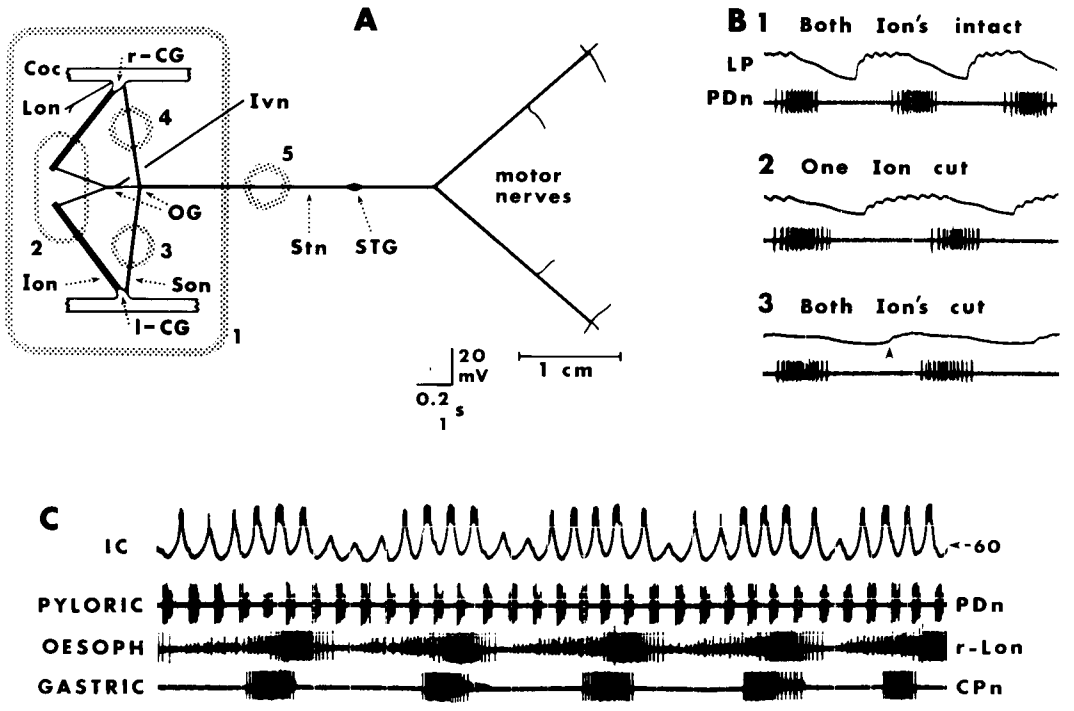

FIG. 1. *A*: scale diagram of combined preparation and solution pools as arranged in vitro. Vaseline-pool borders are stippled. Abbreviations: CG: commissural ganglia, bilaterally paired and lying on the circumesophageal connectives (Coc); Ion: inferior esophageal nerve (paired); Ivn: inferior ventricular nerve (unpaired); Lon: lateral esophageal nerve (paired), travels to the lateral esophageal dilater muscle (muscle 02 of Ref. 31), used to monitor the "esophagus rhythm"; OG: esophageal ganglion, composed of two parts; Son: superior esophageal nerve (paired); STG: stomatogastric ganglion; Stn: stomatogastric nerve (unpaired). "Motor nerves" carry the axons of STG motoneurons to foregut muscles. *B*: nerve-cutting experiments to show that trains of EPSPs in LP from the pyloric P-interneurons (section 1) could be progressively eliminated by cutting each Ion in turn (sections 2 and 3). Intracellular record from LP, hyperpolarized by −4 nA via another electrode, with nerve record of PD-driver firing. Arrow in section 3 indicates onset of reversed IPSPs from PL and PE cells within STG (*G89*). *C*: slow modulation of intracellular activity in the IC pyloric follower neuron, with simultaneous records of three different motor rhythms of the foregut: pyloric rhythm, a nerve record of PD driver bursts; gastric rhythm, a nerve record of CP neuron bursts; esophagus rhythm, recorded from a commissural ganglion nerve (Lon, see diagram in *A*) (*G43*). Upper time calibration applies to *B*, lower to *C*. Voltage calibration applies to LP (*B*) and IC (*C*) intracellular records.

the name of the major neuron type present, followed by an n, rather than by the nerve nomenclature of Maynard and Dando (26); the nerves typically monitored are given in Table 1.

Exclusion of network explanations

Phasic synaptic input to a cell or feedback synaptic interactions between a cell and a network might, in principle, be able to mimic, reinforce, distort, or obscure plateau-type behavior. One approach to excluding "network explanations" for plateau-type behavior was observational in nature: an intracellular event was shown to occur independent of changes in other network activity, monitored in nerve records. This was done in several of the figures by superimposing and comparing a "control" and "test" oscilloscope sweep, both synchronized to a fixed point in the pyloric rhythm (the start of PD bursts). For clarity, the nerve monitors were half-wave rectified so that spikes point "upward" in the sweep designated "1", while in sweep "2" the rectified nerve traces were inverted so that spikes point "downward" on a shared base line. The timing of presynaptic cell firing could then be directly compared in the "control" and "test" situations. The synaptic organization of this 14-cell system has been studied for over 2 decades, so we knew in advance which other neurons were in presynaptic relation to a neuron being tested for plateaus.

Timing tests were another means to exclude network interpretations: an intracellular response was shown to occur independent of stimulus phase in the rhythm. This was useful for the follower

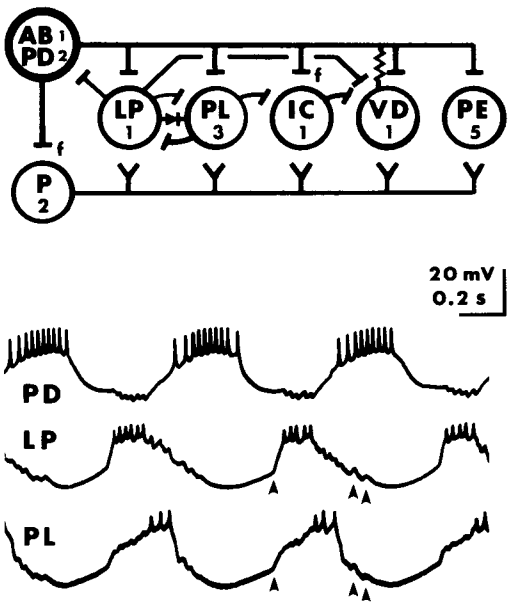

FIG. 2. Synaptic connections and intracellular activity of pyloric-system neurons. Connections are somewhat simplified; f indicates a functional connection; the number of neurons of each type is indicated. PL neurons are electrically coupled to each other; PE neurons can have weak interactions with LP. Simultaneous intracellular records from PD, LP, and PL show the three-part pyloric rhythm, from a combined preparation with moderate activity. Simultaneous EPSPs in LP and PL from the pyloric P-interneurons are visible; a few are indicated by arrows. P-cells also have an "excitatory" input to the PD-AB group, enhancing bursting behavior (*G78*).

neurons, since most have little effect on the cycle period of the pyloric rhythm.

Network interpretations were also excluded in some cases by experimental approaches such as hyperpolarizing presynaptic cells to prevent their firing and synaptic output, nerve section to eliminate the P inputs (below), or blockade of central ganglia to provide unpatterned input to STG (below).

Slow modulation of pyloric activity

There are several ongoing motor rhythms in the combined preparation (31, 37). In addition to the relatively fast pyloric rhythm (0.5–0.7-s cycle period), there are the much slower gastric rhythm and esophagus rhythm (5–10-s cycle periods). The activity level of pyloric-system neurons tended to vary in synchrony with the slow rhythms (Fig. 1*C*). The cycle period of the pyloric rhythm was also modulated (seen better in other examples), which raised problems for delivering constant-phase stimuli.

Comparable activity levels and similar cycle periods were needed for valid comparison of control and test runs, and could be obtained in several ways: *1*) Slow modulation was sometimes weak and could reasonably be ignored; *2*) control and test cycles of the pyloric rhythm could be taken at a fixed phase of the slow modulation, estimated from monitoring both the esophagus rhythm (from the LON—Fig. 1*A*, *C*) and the gastric rhythm (usually from the CPn—Fig. 1*C*); *3*) in two sequential pyloric cycles the first could be used as the control and the second as the test, since pyloric activity was reasonably constant over time spans that were short compared to the cycle time for slow modulation (see Fig. 1*C*); *4*) gastric and esophagus rhythms, and accompanying slow modulation of pyloric activity, could be abolished by bathing the commissural and esophageal ganglia in low-Ca^{2+} saline for 1–2 h (39). Only the pyloric rhythm continued, with activity that was quite steady, although it tended to decline slowly over several hours.

BACKGROUND

Pyloric network

Table 1 enumerates the pyloric-system neurons. The three driver neurons, one AB and two PDs, are endogenous repetitive bursters and supply the basic rhythmicity of the pyloric system (25). They are electrically coupled and burst synchronously. The driver

TABLE 1. *Pyloric network cells and nerves monitored*

Pyloric Cell	Origin	Number	Role	Type		Nerve Monitored
AB	Anterior burster	1	Driver	Interneuron	Stn	Stomatogastric nerve
PD	Pyloric dilator	2	Driver	Motor neuron	PDn	Pyloric dilator nerve
LP	Lateral pyloric	2	Follower	Motor neruon	v-Lvn	Ventral-lateral ventricular nerve
PL	Pyloric-late	3–4	Follower	Motor neuron	PLn	Ampular nerve
PE	Pyloric-early	ca. 5	Follower	Motor neuron	PEn	Distal pyloric nerve
VD	Ventricular dilator	1	Follower	Motor neuron	VDn	Median ventricular nerve
IC	Inferior cardiac	1	Follower	Motor neuron	ICn	Median ventricular nerve
P (pyloric)		2	Follower	Interneuron		

Pyloric P-interneurons are located in the commissural ganglia, others in the stomatogastric ganglion. Terminology is from Refs. 26 and 38.

group periodically inhibits all the pyloric follower neurons (Table 1), as can be seen in Fig. 2 (inhibitory postsynaptic potentials (IPSPs) and hyperpolarization in the lateral pyloric and pyloric-late (LP and PL) follower neurons correspond to the times of the PD bursts). The diagram in Fig. 2 of synaptic connections among pyloric-system neurons is simplified for purposes of this paper (17, 25, 27). The chemical synapses are all inhibitory, except those from the P inputs.

The pyloric follower neurons are diverse in synaptic connections, cellular properties, and phasing in the pyloric rhythm. Note in Fig. 2 that LP fires a burst before PLs to form a three-part sequence, PD-LP-PL. The termination of LP firing is aided by powerful IPSPs from the PL group (18, 19) (Fig. 2). The weak LP → PL inhibition appears to act in concert with cellular mechanisms of PL neurons to delay the PL firing (16, 18).

Besides the 14 neurons in the STG, the central pattern generator for the pyloric rhythm also includes at least two additional neurons in the commissural ganglia. The P-interneurons burst with the pyloric rhythm, are inhibited by an ascending axon from the AB driver interneuron, and at least two of them feed back to evoke trains of excitatory postsynaptic potentials (EPSPs) in pyloric-system neurons of STG (36–38). This phasic excitation is synchronous with bursts in the STG follower neurons (arrows, Fig. 2). It was desirable to eliminate the P inputs to STG in order to minimize network interactions. This could be done in about half the attempts by cutting or sucrose blocking the inferior esophageal nerves (38) (Ion, Fig. 1*A*), which could block the descending axons from the P inputs but leave intact other activating inputs to STG traveling through the superior esophageal nerves. The blockade procedure was done while recording intracellularly from a follower STG cell, looking for the disappearance of EPSPs with the cell hyperpolarized (Fig. 1*B*). Usually all the STG follower neurons continued to burst vigorously despite eliminating the P inputs.

RESULTS

The behavior of selected follower cells (usually the LP cell) is compared in a systematic way to slow regenerate behavior of the PD-AB driver cells summarized in Fig. 4, since these are already known to burst endogenously (25, 42). Some examples of regenerative behavior in the other types of follower neurons are then presented.

Lack of phasic synaptic input during follower-neuron bursts

Provided the P inputs have been eliminated, there is little or no documented synaptic input (phased to the pyloric rhythm) to most follower neurons that could explain the onset and driving of their bursts. Figure 3*A* shows that no discrete synaptic potentials were visible in a hyperpolarized LP cell during the normal burst time, until late in the cycle when the prominent PL → LP inhibition started (arrow).

Since the burst onset in follower neurons was of major interest, resistance measurements were made during the "silent period":

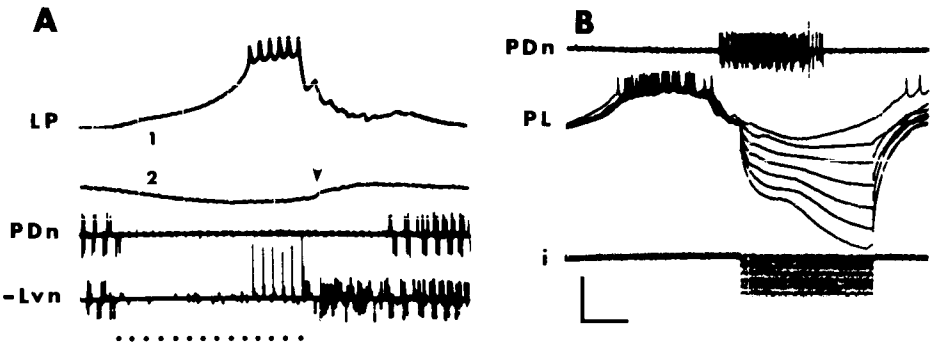

FIG. 3. *A*: dotted line indicates phase of follower-cell cycle lacking any known synaptic input from other pyloric-system neurons. LP cell, with Ion's cut to eliminate P inputs. A normal burst, 1, and a hyperpolarized sweep, 2; offset = −4 nA, were superimposed. Arrow, onset of IPSPs from PL cells. v-Lvn trace shows firing of PD, LP, PL, PE, and other cell types. *B*: PL cell; hyperpolarizing pulses started during the inhibitory barrage from the driver group and continued through most of the PL interburst interval. Top trace is control. Calibrations: *A*: 10 mV, 0.1 s. *B*: 20 mV, 5 nA, 0.1 s. Note smoothness of voltage trajectories during time indicated by dotted line.

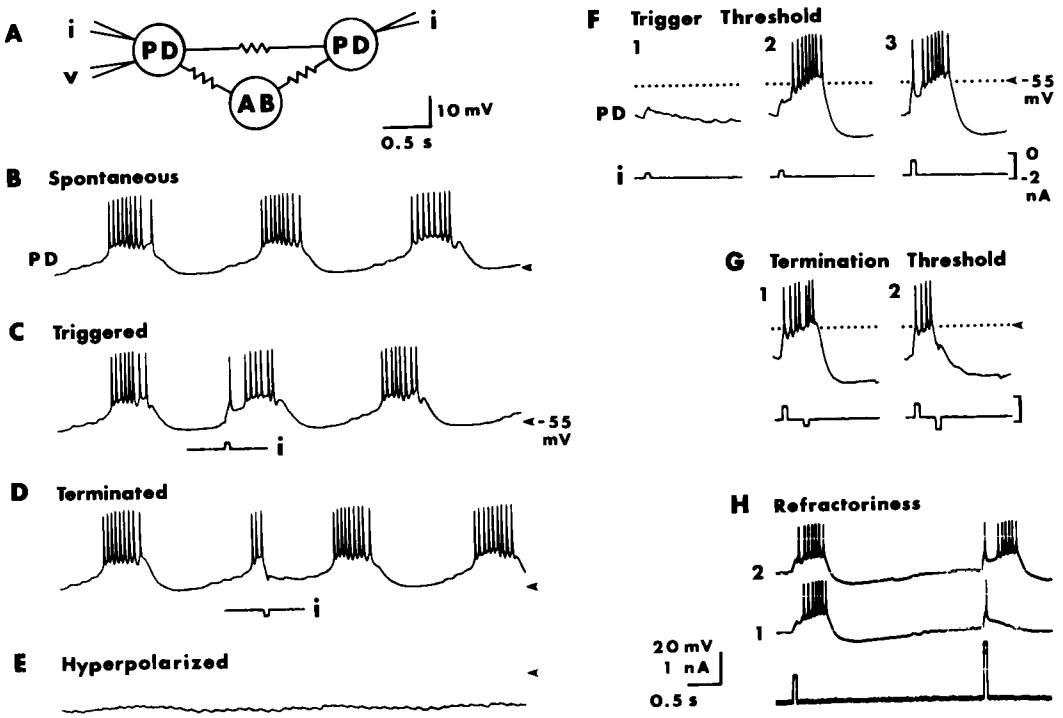

FIG. 4. Plateau properties of the driver group. The preparation included only the STG and esophageal ganglion. *A*: experimental arrangement. Current electrodes (i) were placed in both PD cells, with a recording electrode (v) in one. Equal currents were injected into each PD cell, but calibrations for bath current monitor (*F* and *H*) are referenced to current passed into one PD cell. Voltage responses represent behavior of the three electrically coupled PD and AB cells. *B–D*: no offset current was used. *B*: spontaneous bursting. *C*: premature triggering. *D*: premature termination. *E–G*: a steady hyperpolarizing offset of −1.6 nA was applied, which stopped spontaneous bursting (*E*). F_1–F_3: depolarizing pulses of increasing strength were given; the stronger ones triggered bursts. *G*: a triggered burst was only momentarily interrupted by a −0.5-nA hyperpolarizing pulse (G_1) but was terminated by a stronger pulse (G_2, −2.0 nA). *H*: although a depolarizing pulse (0.8 nA) did trigger a burst, 3 s later a much stronger pulse was needed (H_2, 1.6 nA), since a slightly weaker second pulse failed (H_1, 1.4 nA). Offset was −1.8 nA. Time and voltage calibrations in *A* and current calibration in *F* apply to *B–G*. Arrows in *B–G* indicate −55 mV. All pulses were 50 ms duration (*G61*).

the 200–400 ms when the follower neurons are hyperpolarized and nonfiring following the barrage of IPSPs associated with a burst in the driver group. The results in Fig. 3*B* are interpreted as showing a net conductance increase during the driver inhibition, decaying relatively rapidly to a much higher input resistance and more-or-less passive behavior (at these negative V_m levels) during the silent period in a PL neuron. Some neurons, such as PLs, do receive inhibition during the silent period, but it is weak (17) and its elimination by pharmacological blockade has little effect on the phasing of PL bursts (4). In general, the silent period in the follower neurons appears to mainly be under the control of cellular mechanisms, with little or no synaptic input from other STG neurons.

Large membrane-potential oscillations

All the neurons show large excursions in membrane potential during brisk activity of 10–25 mV, typically about 20 mV, measured from the most negative point ("trough") to the base of spikes ("peak"). This is seen in Fig. 4*B* for a moderately active PD cell and in Fig. 3*A* for a highly active LP cell, etc. Large excursions in membrane potential (exclusive of spikes) must be present in some region of a cell if a voltage-dependent plateau-type of mechanism is to operate.

Burst suppression by hyperpolarizing currents

In all neurons, a steady hyperpolarizing current of sufficient strength had the effect

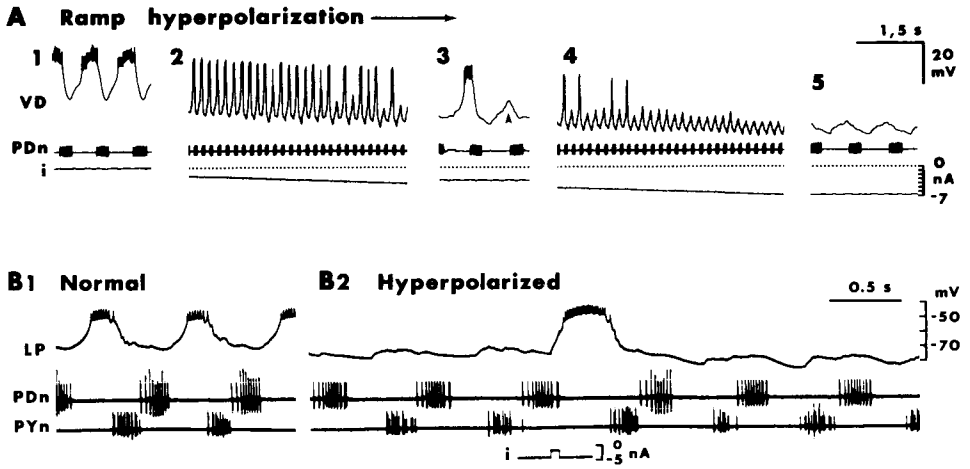

FIG. 5. Effects of hyperpolarizing offset current. *A*: a slow ramp of increasing hyperpolarizing current (i) was injected into a VD cell through a double-barrel microelectrode. The PDn trace monitored the driver-group rhythm. Sections 1, 3, and 5 are expanded records (*G24*). B_1: spontaneous LP bursting, with simultaneous nerve records of PD (PDn) and PL + PE (PYn) firing. B_2: LP bursting was suppressed by a −4-nA offset, but a burst could be triggered by a 2-nA 50-ms pulse. Note that the phase of PY bursting, relative to the PDn bursts, was little changed with LP shutoff (B_2 compared to B_1) (*G49*).

of suppressing bursts and eliminating or reducing the amplitude of oscillations. Figure 4*E* illustrates this for the PD/AB cells; hyperpolarization stopped all oscillations, consistent with their role of "driving" the pyloric rhythm. While hyperpolarization of a follower cell did not stop the rhythmicity in other cells, it did greatly reduce the amplitude of oscillations in the polarized cell; the remaining smaller oscillations appeared to be synaptic in origin.

The important feature is the abrupt, nongraded manner in which the follower-neuron bursts dropped out. As the ventricular dilator (VD) cell in Fig. 5*A* was increasingly hyperpolarized by a ramp current, the amplitude of oscillations initially increased due to the trough moving more negative than the peak. With stronger current, abrupt drops in amplitude began to occur intermittently (sections 2 and 3) associated with failure of bursts. Further hyperpolarizations increased the proportion of cycles in which "all-or-none"-like failures occurred (section 4). This is evidence for a slow threshold- and voltage-dependent process in the follower neurons, as in other excitable systems (cf. Ref. 34).

If a strong hyperpolarizing current was steadily applied, a follower cell would eventually appear to adapt to it and start to show intense "escape" bursts at long intervals. These had a longer duration and higher spiking rate than normal bursts. Another response to offset currents were the sharp peaks superimposed on the periodic synaptic input at intermediate levels of hyperpolarization (arrow, Fig. $5A_3$), appearing much like "local responses" in nerve (20). They were voltage dependent since they disappeared with further hyperpolarization (Fig. $5A_5$). Also, in all the follower cells a long relatively weak current pulse that straddled the normal burst time could sharply reduce the oscillation amplitude. The reduction in amplitude was much more than expected from the passive charging seen during the silent period at the start of the pulse, again consistent with keeping the cell below a voltage threshold.

Triggering bursts

In regularly bursting cells, both drivers and followers, a brief depolarizing-current stimulus applied in the interburst interval would trigger a burst depolarization "prematurely"—i.e., before the expected time of burst onset. This is shown for the driver cells in Fig. 4*C* and for the LP follower cell in Fig. 6*A*. The pulse caused LP to fire four extra spikes before the normal burst onset. The amount of burst advance was graded with the pulse strength (Fig. 6*B*) and, therefore, the premature triggering was not an all-

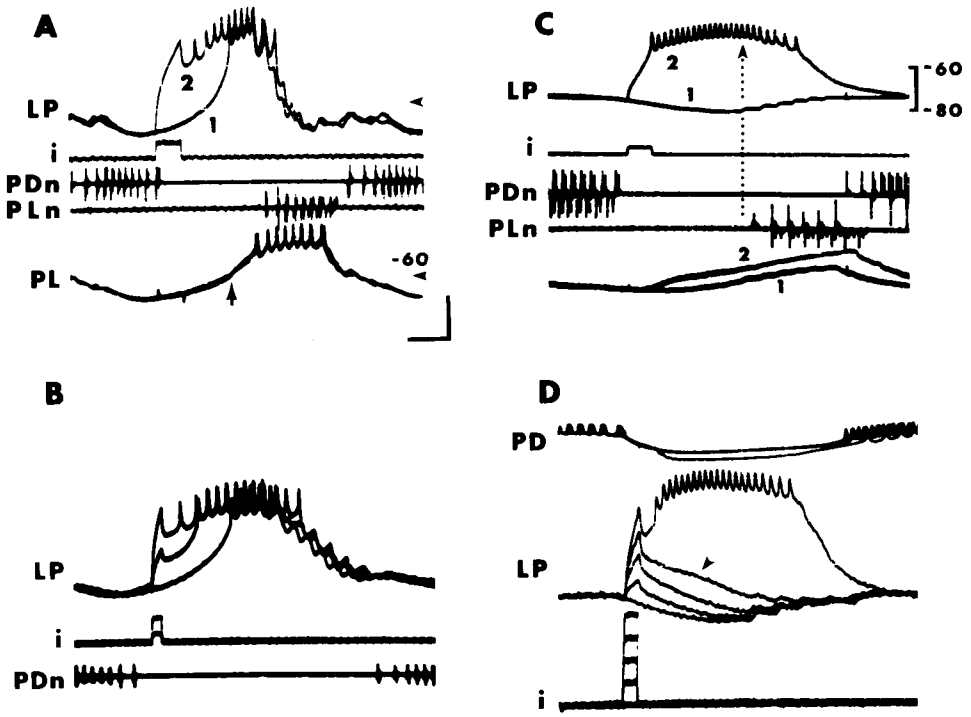

FIG. 6. Triggering bursts in LP cell with current pulses. *A*, *B*: premature triggering, no offset current applied. *A*: the network was monitored in nerve records and simultaneous records from a PL cell along with LP; vertical arrow indicates onset of P-input EPSPs. Successive control, 1, and test, 2, cycles were superimposed. Both horizontal arrows = −60 mV (*G42*). *B*: burst advance was graded with current intensity; three cycles were superimposed, with a PDn record from one; P inputs were eliminated; all cycles were at identical phase of the esophagus rhythm (*G52*). *C*, *D*: burst triggering in hyperpolarized LP cells. *C*: triggered burst, with network monitors; LP offset, −5 nA; pyloric P inputs were eliminated. Control cycle, 1, immediately preceded test cycle, 2. Vertical dotted line shows time of first PL spike in control cycle, corrected for conduction delay (*G52*). *D*: threshold demonstration; LP offset, −6 nA, with no escape bursting; the pyloric P inputs were eliminated; the commissural and esophageal ganglia were bathed in 0 Ca^{2+}-2 × Mg^{2+} saline to eliminate slow modulation, so that the LP excitability was constant. Weak pulses were followed by passivelike decay to base line: near-threshold pulse appeared to evoke a partial active response (arrow). Voltage calibration: 10 mV for LP in *A*, *B*, *D*; 20 mV for PL in *A*, and LP in *C*. Current calibration: 10 nA for *A*, *B*, *D*; 20 nA for *C*. Time calibration: 0.1 s.

or-none process. Similar graded premature triggering is seen in the repetitive spiking of neurons and cardiac muscle (21, 53).

Burst triggering acquired an all-or-none character when a cell was otherwise held silent by a steady hyperpolarizing current, as seen in Fig. 4*F* for the driver cells and in Fig. 5B_2 and 6*C* for the LP follower cell. In Fig. 5B_2, a brief depolarizing pulse given in the normal silent period elicited a large depolarizing wave and high-frequency firing of the LP axon, with relatively little perturbation of rhythmicity in the other network cells (PDn and PYn traces). Triggered bursts were longer in duration and had higher spiking rates than normal bursts. The V_m level reached during the prolonged depolarization was nearly the same in Fig. 5B_1 and B_2; since the trough V_m level was held more negative by the injected current, the amplitude of triggered bursts was quite large, e.g., 30–40 mV. There was a threshold of current intensity required to trigger a burst (Fig. 6*D*). There was a strength-duration trade-off for the stimulus needed to trigger a burst. Triggered bursts outlasted the (passive) trajectories to subthreshold pulses (Fig. 6*D*). Cells showed metastable-like behavior at pulse intensities near threshold (22) (Fig. 6*D*, arrow; Fig. 7A_2). Responses showed growth after just-suprathreshold stimuli (Fig. 7*B*, weakest pulse). Responses showed stimulus independence, since once the burst started the spike frequency envelope and the V_m level of the peak

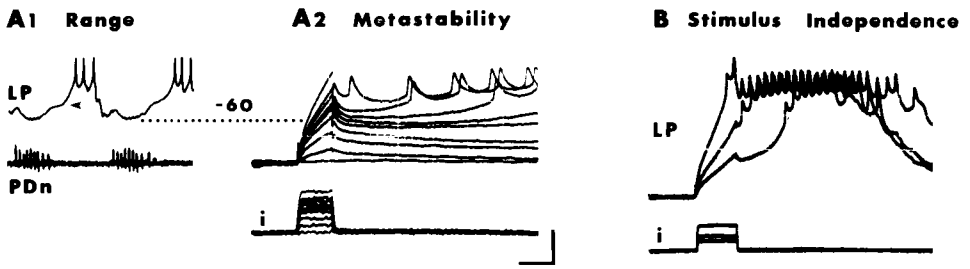

FIG. 7. Properties of burst triggering in LP. *A*: operating range and metastability. Only the left-superior esophageal nerve was intact; the pyloric P inputs were eliminated; the commissural and esophageal ganglia were blocked by 0 Ca^{2+}-2 × Mg^{2+} saline to stop slow modulation. A_1: spontaneous activity, no offset. Arrow indicates inflection. A_2: same LP cell, showing threshold for triggering with −3.5 nA offset. From lower to upper, the fourth and fifth stimuli evoked prominent metastable trajectories. Dotted line, −60 mV for A_1 and A_2 (*G80*). *B*: triggering bursts in hyperpolarized LP cell; offset, −3.5 nA. For all three bursts, the firing rate followed a similar parabolic envelope, and the peak V_m level was similar (*G43*). In both A_2 and *B*, stimuli were given just after driver group bursts. Voltage calibration: 10 mV. Current calibration: 5 nA in A_2, 10 nA in *B*. Time calibration: 300 ms in A_1, 20 ms in A_2, 50 ms in *B*.

tended to be independent of the pulse strength (Fig. 7*B*); the major effect of increasing the pulse strength (at constant duration) was a decrease in the latency before the start of a burst. All this behavior appeared much like the triggering of a voltage-dependent regenerative wave, as in the driver cells (Fig. $4F_{1-3}$) and many other excitable systems.

Figure 7*A* also illustrates that the threshold level, defined by the metastability in section 2, fell within the normal operating range of membrane-potential excursion seen in section 1 (applying small corrections for passive *I-R* distortion of V_m levels in A_2). This means that the threshold V_m level lay positive to the normal oscillation trough and negative to the normal oscillation peak, as required if a voltage-dependent mechanism is to drive the normal prolonged depolarization. Furthermore, we interpret the inflections of V_m during normal bursting (arrow, Fig. $7A_1$) as another indicator of threshold: the transition from passive recovery to activation of regenerative processes. The premature triggering during normal oscillations (as Fig. 6*A*) is additional evidence for a regenerative plateau mechanism being activated within the normal operating range.

Terminating bursts

Bursts could often be terminated abruptly by brief hyperpolarizing pulses of sufficient intensity. This held true for spontaneously initiated as well as pulse-triggered bursts, in nonpolarized as well as hyperpolarized cells, and in driver cells (Fig. 4*G*) as well as follower cells.

Premature termination of normal bursts in the LP follower cell is shown in Fig. 8*A*, comparing a control burst, 1, with a test burst, 2, in which a brief hyperpolarizing pulse was given soon after the start of LP firing. Four LP spikes were abolished after the pulse compared to the control. Termination exhibited thresholdlike characteristics (Fig. 8*B*). A pulse that was too weak could result in rapid depolarization and "reignition" of the burst (trace 1), whereas a slightly stronger pulse caused termination (trace 2). A pulse of fixed near-"threshold" intensity could evoke either response (inset, Fig. 8*A*).

Termination was more readily demonstrated for the long intense bursts elicited in hyperpolarized cells (Fig. 8*C*). Once triggered, there was a threshold for termination (Fig. 8*D*). The threshold current strength for repolarization varied over the course of the burst, as shown in Fig. 8*E* for just-suprathreshold currents at three delays after triggering a burst. The data plotted in Fig. 8*F* show that the threshold initially increased, which paralleled the observation that LP continued to depolarize and its firing rate accelerated at the beginning of an evoked burst (see Fig. $8C_1$). Threshold declined thereafter, probably due both to cellular properties and also to incoming synaptic inhibition from the PL group. There was a trade-off between strength and duration of the hyperpolarizing pulse required to terminate a burst, as seen in Fig. 11*B* for three different near-threshold pulses. Note that the V_m level reached by all three was comparable.

Burst termination in the follower cell re-

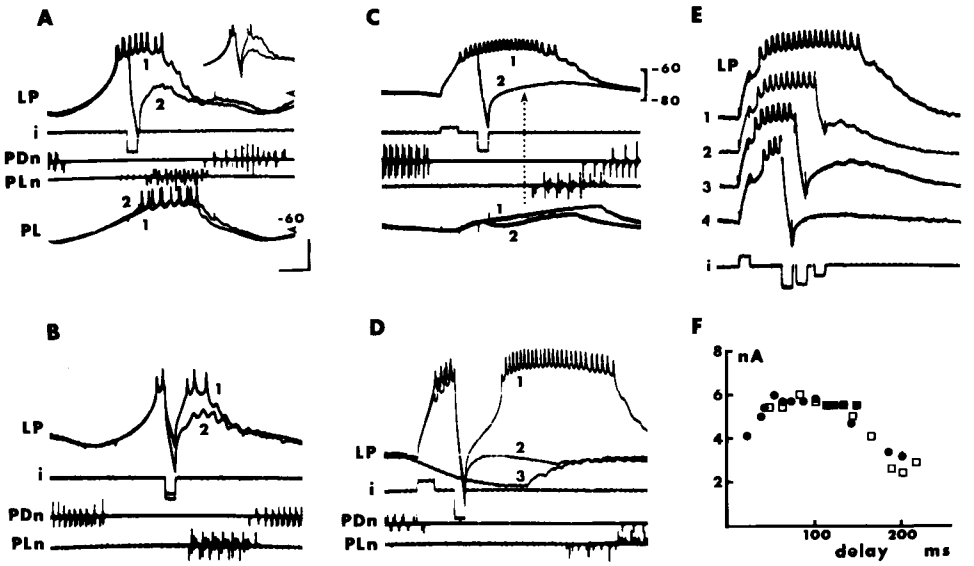

FIG. 8. Terminating bursts in LP cell with current pulses. *A*, *B*: stimulation during normal bursts, not applying any offset current. *A*: premature termination, with network monitors such as simultaneous intracellular record from a PL cell along with LP; control cycle, 1, immediately preceded test cycle 2. Horizontal arrows, −60 mV (*G52*). *B*: threshold demonstration; cycles 1 and 2 were taken at same phase of esophagus rhythm. *C–F*: data from hyperpolarized LP cells. *C*: termination example with nerve monitors; control cycle, 1, immediately preceded test cycle, 2. Vertical dotted line shows time of first PL spike in control cycle, corrected for conduction delay (*G52*). *D*: threshold for termination; identical pulses were given for traces 1 and 2; a nonperturbed base line trace, 3, is also shown; cycle 1 immediately preceded cycle 2 (*G52*). *E*: termination delay series; the 35-ms hyperpolarizing pulses in traces 2–4 were just sufficient to cause repolarization. Precautions to ensure constant excitability of LP included bathing the commissural and esophageal ganglia in 0 Ca^{2+}-2 × Mg^{2+} saline to eliminate slow modulation, triggering bursts regularly every 5 s, and spacing the termination tests between two to four triggered bursts. Only one superior esophageal nerve was intact, to have more moderate activity (*G84*). *F*: threshold for repolarization versus delay of hyperpolarizing pulse from the first spike in burst, from same data as *E*. Filled circles: the burst was terminated. Open squares: reignition of burst (*G84*). LP offsets: *C* and *D*, −5 nA; *E* and *F*, −4 nA. The pyloric P inputs were eliminated for all panels. Voltage calibration: 10 mV for LP in *A*, *B*, *D*, *E*; 20 mV for PL in *A*, and LP in *C*. Current calibration: 10 nA for *A*, *B*, *D*, *E*; 20 nA for *C*. Time calibration: 0.1 s.

sembled the regenerative repolarization described in axons, cardiac muscle, etc. (13, 45, 53), in which it represents a threshold-dependent regenerative transition from the "high" to the "low" state and is the inverse of response triggering. Note in Fig. $4G_2$ that regenerative repolarization in a PD cell brought the V_m level to only about the level existing initially; it seems that another type of cellular repolarization mechanism underlay the rest of the postburst hyperpolarization in the driver cells.

Possible network interpretations

The driver cells (Fig. 4) were tested under conditions in which most other network cells were hyperpolarized and not firing, so that network interactions were minimal.

Could the synaptic connections of the LP cell be responsible for its "regenerative-like" behavior? Possible network explanations had to be considered, since the LP cell was tested under conditions of high activity throughout the network, since LP forms reciprocal inhibitory networks with the driver cells on the one hand and with the PL follower cells on the other hand (Fig. 2), and since feedback networks are often invoked as a possible basis for oscillations (cf. Ref. 7). In the case of premature triggering of LP bursts (Fig. 5*A*), monitoring the network sufficed to rule out such arguments. Comparing the control (trace 1, upward spikes) and test (trace 2, downward spikes) cycles, it can be seen that premature triggering of the LP burst was not associated with significant perturbation of activity in the PDs (PDn nerve monitor), nor in the PLs (PLn nerve monitor and PL intracellular), nor in the P-cells (arrow). The premature triggering was made at a phase at

which LP receives little if any synaptic input from the pyloric network (cf. Fig. 3). Other possibilities, such as fluctuation in cell excitability, were specifically minimized (METHODS). The premature triggering was apparently due to an intrinsic cellular property of the LP cell.

Stimulating early in the silent period was again useful for analyzing the triggered bursts in hyperpolarized LP cells. At least the initial 210-ms portion of the triggered burst in Fig. 6*C* (preceding the dotted arrow) could not be attributed to any change in firing of the PL or PL groups, since they are normally hyperpolarized and nonfiring at this early phase.

Figure 9 shows that LP and VD bursts could be triggered at a wide range of phases in the pyloric cycle. This was another way of demonstrating that triggered bursts were produced endogenously, since they were independent of network interactions occurring at a given phase in the cycle. The ability to trigger regenerative plateaus in a given cell can be expected to depend on the types of synaptic interactions involved. For example, the low percentage of successful triggers for stimuli at late phase (Fig. 9A_3) and very early phase (9A_4) can be attributed to inhibitory input to the LP cell from the PL group and the driver group, respectively. By contrast, the VD follower cell does not receive inhibitory input at late phase, and indeed its bursts could be triggered very late in the cycle (Fig. 9B_3, B_4). The tendency for VD triggering to fail near phase = 0.3 (B_4, line F) can be attributed to the electrical coupling of VD to the driver group, since the PD-AB driver cells are repolarizing at this phase.

The late part of a triggered LP burst and the effect of hyperpolarizing pulses to prematurely terminate LP bursts were more problematical due to the LP $\rightleftharpoons$ PL reciprocal inhibitory network, since the PL cells start to fire toward the end of LP bursts. For example, the endogenous nature of the later part of the triggered LP burst in Fig. 6*C* might be considered equivocal since the LP $\rightarrow$ PL and LP $\rightarrow$ PD inhibition, reflected in the delay of PL and PD bursts in the test cycle (downward spikes), undoubtedly did permit a longer LP burst. Similarly, the powerful

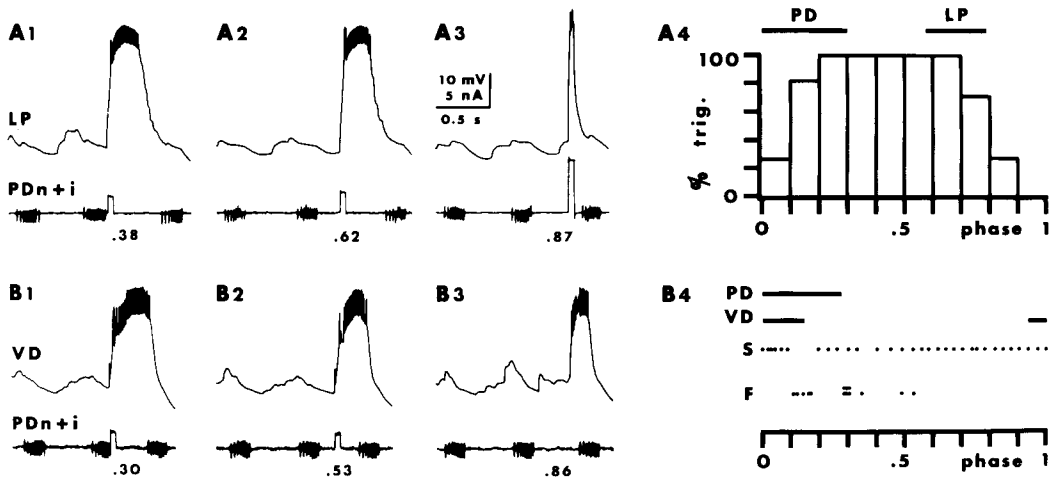

FIG. 9. Triggering ability versus cycle phase. A_{1-3}: LP data; offset, −4 nA; numbers below panels give phase of current pulse, referenced to preceding cycle. Note failure to trigger at late phase (A_3) even with a stronger pulse. A_4: LP cell data from several runs with different offsets and pulse amplitudes were grouped. The start of PD bursts = phase 0 and 1; phase values were corrected for conduction delay of PDn. Ordinate: percentage of current pulses in a given phase bin that evoked burst = two or more spikes afterward. Horizontal bars: measured average phase of normal PD and LP bursts in this preparation. Stimuli given during the start and middle of PD bursts did evoke bursts, but bursts were delayed in onset until after the driver burst ended (*G43*). B_{1-3}: VD data; offset, −4 nA. B_3: spontaneous EPSPs triggered burst. B_4: one-dimensional graph shows corrected phase of triggering stimuli, from pooled VD cell data. s, successful triggering trials, by either current pulses or EPSPs, selected to cover the whole range of phase. f, failures to trigger by current pulses, incuding all available data. Horizontal bars show measured average phase of normal PD and VD bursts in this preparation (*G24*).

PL → LP inhibition might have caused or "reinforced" the termination of LP firing once the LP firing was interrupted by a hyperpolarizing pulse. However, we could find examples in which terminating an LP burst with a current pulse was accompanied by little change in the number and timing of PL spikes (Fig. 8*B*). Also, bursts could be terminated well in advance of the normal onset of PL firing (120 ms in Fig. 8*C*, 330 ms in Fig. $8D_2$); for this time at least, PL inhibition was unlikely to have been a factor.

"Nonspiking" network interactions from the PL or PD groups could, in principle, be affected by the LP plateau. In particular, LP inhibition of these cells could suppress possible ongoing release of inhibitory transmitter back onto LP, thus potentiating the LP burst. However, LP plateaus could be triggered or terminated at points of the cycle (e.g., the silent period) at which nonspiking input is expected to be minimal, i.e., when PDs and PLs are near the trough of their oscillations (see Figs. 2 and 6*A*). It has been shown that there is relatively little nonspiking release from pyloric-system neurons when near rest (14).

We often polarized presynaptic neurons to test the effect of certain synaptic connections on plateaulike behavior. Strong hyperpolarization was effective in abolishing synaptic output effects from a presynaptic cell, as judged by the abolition of its firing and the disappearance of IPSPs and other perturbations of postsynaptic activity. *1*) A typical example was LP → VD inhibition, which was strong enough to delay or interrupt firing of the VD follower cell (cf. Figs. $12A_1$ and 14*A*). With the presynaptic LP cell inactivated by hyperpolarization, normal-amplitude bursts and plateaulike responses such as burst triggering, threshold, etc., continued in the VD cell in a usual manner. The only difference was the absence of a pause or delay associated with (normal) LP time. *2*) Likewise, hyperpolarization of VD (which may indirectly weakly affect other follower cells; Ref. 18) had little effect on plateaulike responses in LP, IC, etc. *3*) Hyperpolarizing LP had little effect on the phasing of bursts in the PL follower group (Fig. $5B_2$) (confirming that LP → PL inhibition is not the primary cause of the delayed bursts in PL cells; Refs. 7, 23). *4*) In one case, three of four PL cells were impaled and strongly hyperpolarized, yet normal burst depolarizations continued in the LP cell. *5*) We have previously reported that repetitive LP bursts continued when the driver group was strongly hyperpolarized to remove their influence and under conditions when the PL group was not bursting; the LP ⇌ driver as well as the LP ⇌ PL networks were, therefore, apparently not contributing to the continued LP bursting, which then was probably due to endogenous mechanisms (41).

The P inputs probably tend to trigger and excite bursts, but they are not necessary for near-normal burst amplitude, burst phasing, and the spectrum of regenerative-like responses, since these continued in all the various STG follower cells in preparations with the P inputs eliminated by cutting or blocking certain connectives (BACKGROUND) (Figs. 3*A*, 4, 6*B–D*), 7*A*, 8, 11*A–C*, 13*A*, 14*A*, $15B_2$). That regenerative-like responses were not due to indirect synaptic pathways through the higher level ganglia was confirmed in experiments of abolishing synaptic transmission and recordable phasic or rhythmic activity in the higher level ganglia by bathing them in low-Ca^{2+} media; regenerative-like responses continued in follower cells such as LP (Figs. 6*D*, 7*A*, 8*E* and *F*, 13).

In summary, the network of (inhibitory) synaptic connections in the pyloric generator seems to affect mainly the repolarization phase in the follower neurons.

Comparison to passive model

One model for follower-cell activity assumes that, within a pyloric cycle, a follower cell would be inhibited by the driver group and then relax in a passive *R-C* manner (perhaps aided by postinhibitory rebound) to approach asymptotically a more positive level above the threshold for spiking. Could this model mimic LP behavior? To test the model in a semiquantitative way, we have compared the responses of a simple cable (Fig. 10*A*) to the responses of the LP cell to current pulses given in the interburst interval (Fig. 6*B*). In the cable, a long current pulse representing synaptic inhibition by the driver group (I_s) was applied to the "dendritic" end while brief "test pulses" (I_t) were applied at the "soma" end, corresponding to the unipolar structure of these crustacean moto-

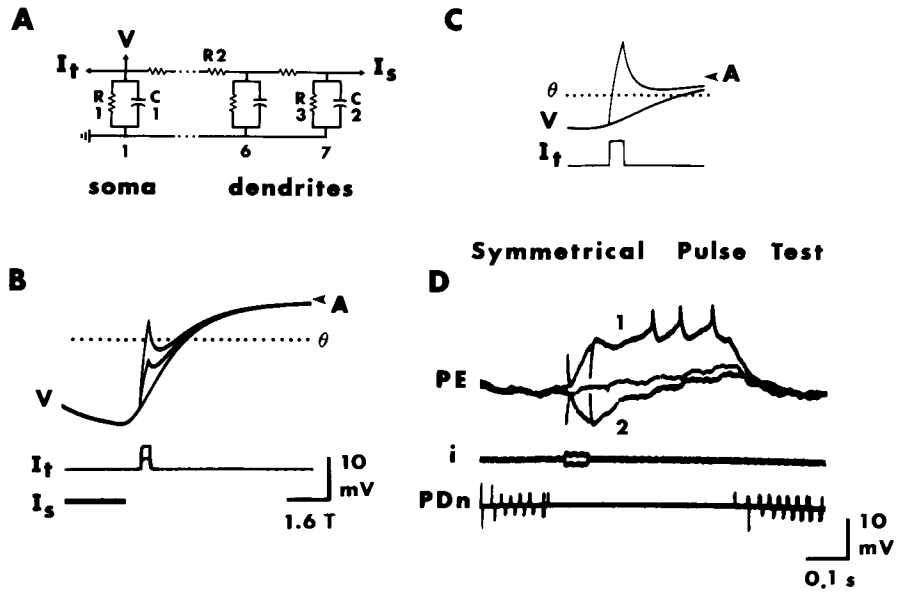

FIG. 10. Cable model and passive behavior. *A*: the cable model consisted of seven compartments, with larger components in no. 7 to simulate the distal dendrites. R1, 47 kΩ; R2, 4.7 kΩ; R3, 6.8 kΩ; C1, 1 μF; C2, 7 μF. *B*: simulation of premature triggering, to be compared directly with LP data in Fig. 6*B*. A long negative pulse (I_s) to the dendrite end of the cable simulated driver-group inhibition, and afterward the voltage (V) decayed back to the asymptote (A). θ = spike threshold. Positive test pulses (I_t) were given to the soma end of the cable model, whose amplitude were adjusted to make the voltage transients in *B* comparable to those in Fig. 6*B*. As explained in the text, the model display was scaled to 1.6 time constants per time calibration, matching the LP display in Fig. 6*B*. The model and cell were also matched for voltage excursion. *C*: cable response to a larger pulse, on a faster time base. *D*: symmetrical positive and negative pulses were given at constant phase to a hyperpolarized PE cell; also superimposed is a nonperturbed trace to show the base line; PE offset, −0.9 nA.

neurons (24). Voltage excursions in Fig. 10*B* for the model were matched to those of the LP records in Fig. 6*B*, conservatively setting the asymptote (A) at 10 mV above "threshold" for spiking (θ). Displays of cable responses (Fig. 10*B*) and cell responses (Fig. 6*B*) were both scaled at about 1.6 time constants per horizontal division (the time constant of an LP cell for weak hyperpolarizing pulses given in the interburst interval was about 60 ms; not illustrated).

The cable model did allow premature triggering of bursts, since a strong depolarizing pulse would sufficiently discharge the cable capacitance to cause a permanent crossing of threshold (Fig. 10*C*). Premature burst triggering is therefore not necessarily by itself a distinguishing sign of regenerative behavior. However, premature triggering of cable model (Fig. 10*B*) and the LP cell (Fig. 6*B*) differed in several respects: *1*) after the "driver inhibition," the cable relaxed quickly to threshold whereas the normal LP burst was delayed; *2*) the recovery trajectory of the nonperturbed model was concave-downward, whereas the LP trajectory leading to the first spike was concave-upward or "accelerating"; *(3)* the model trajectories quickly converged after test pulses, whereas the LP trajectories diverged.

Most other behavior of prolonged depolarizations in the follower cells was qualitatively incompatible with the "passive" model, such as the existence of a threshold for all-or-none triggering or terminating, growth of responses after a current pulse, and the other signs of regenerativeness. An example is that responses often outlasted the perturbing stimulus by substantially more than would be expected of passive responses. This was obvious in cases where strong burst depolarizations were triggered in hyperpolarized silent cells (cf. Fig. 6*C*). For weaker responses, it could be seen by comparing the effects of equal depolarizing and hyperpolarizing current pulses, as illustrated in Fig. 10*D* for a PE cell. The asymmetry is interpreted as an active response evoked by depolarization,

compared to the passive response to hyperpolarizing current, as in other systems (20). It is worth cautioning that other cellular mechanisms, such as a g_A mechanism (6, 16), might also contribute to response asymmetry.

Trajectories and I-V relations

Certain characteristic waveforms and membrane-potential trajectories were difficult to explain in terms of the known network interactions, or passive cellular properties alone. Figure 11 shows cases in which hyperpolarizing current pulses were given during ongoing prolonged depolarizations. A low-intensity current appeared primarily to evoke a passive charging trajectory, since the response saturated and was concave-upward (Fig. 11*A*, −4.8-nA trace). With slightly stronger pulses, the initial rapid charging gave way to a concave-downward trajectory that was "accelerating" in shape, since it became increasingly steep. The accelerating repolarization and the threshold-like behavior are readily interpreted in terms of a voltage-dependent mechanism. The pulse length was restricted to avoid overlap with incoming synaptic inhibition at later phase, but in the absence of network interactions we would expect the trajectory for suprathreshold currents to later become concave-upward again, representing passive charging with a longer time constant in the negative-to-threshold range of membrane potential, as for similar trajectories seen during prolonged active responses in squid axon (1).

A hyperpolarizing pulse that was not sufficiently strong to cause termination was followed by a characteristic sigmoidal depolarizing trajectory leading to resumption of firing (Fig. 11*C*, traces 3 and 4). This appeared much like the accelerating trajectory leading

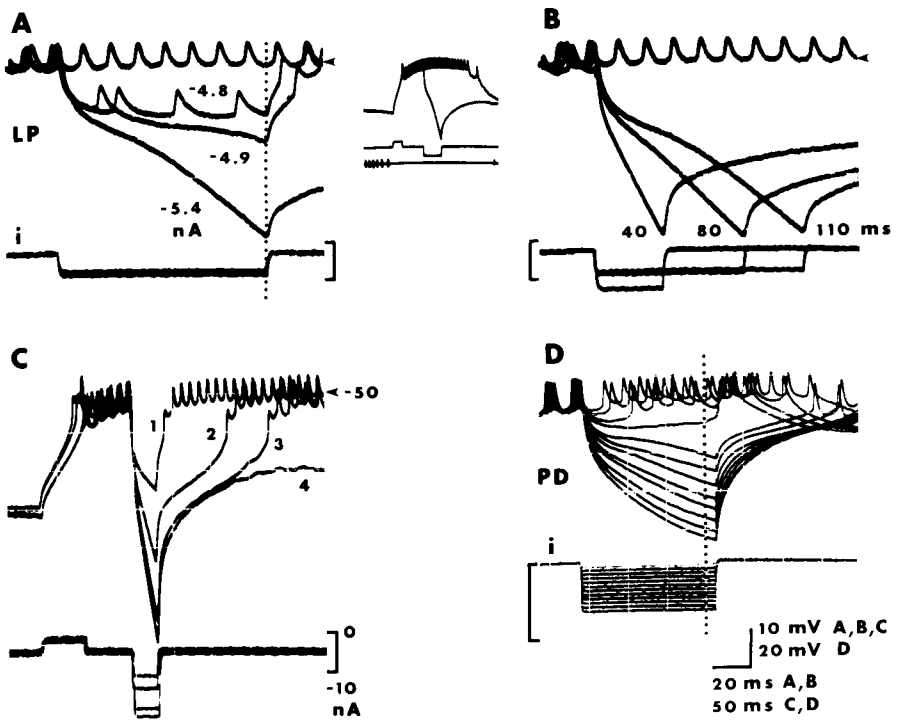

FIG. 11. Repolarization trajectories. *A–C*: hyperpolarized LP, triggering a burst just after the driver burst (as in inset for *A* and *B*) and then interrupting it with a hyperpolarizing pulse. Four sweeps were superimposed. Pyloric P inputs were eliminated (*G52*). *D*: ongoing bursts in PD cells (no offset) were interrupted by hyperpolarizing pulses. Equal currents were injected into both PD cells, but the current monitor is calibrated as current into a single PD cell. Combined preparation. Note abrupt change from concave-upward to concave-downward trajectories in traces 4 and 5 (from upper and lower) and passive character of trajectories to strongest pulses (*G47*). Arrows in *A–C* indicate −50 mV. Current calibrations all show zero level (upper end) and −10 nA (lower end) to indicate offsets in *A–C*.

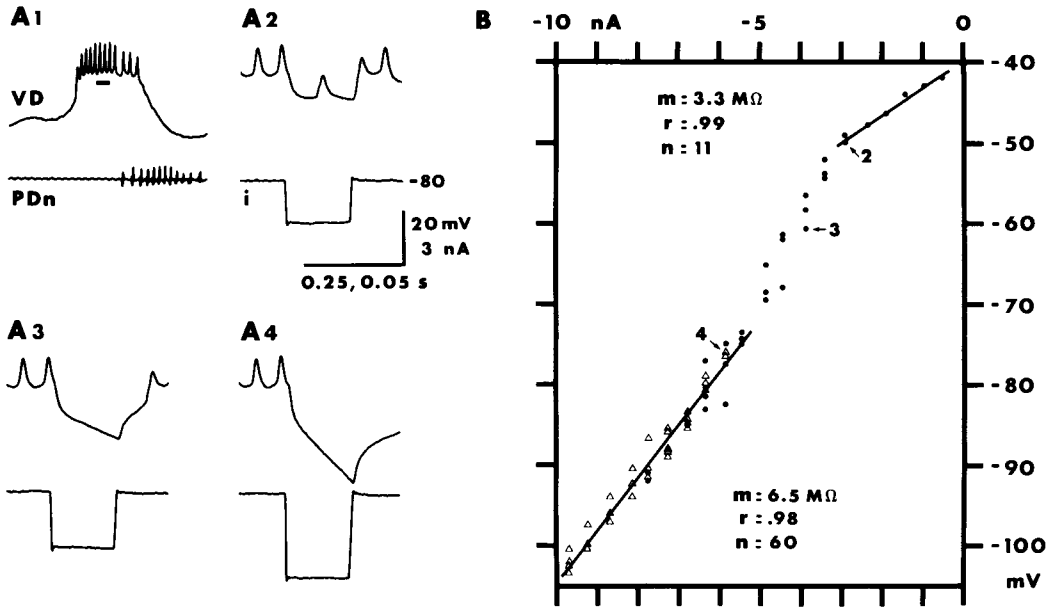

FIG. 12. Nonlinear *I–V* relation for VD cell. *A*: records were made with 4× speed reduction in tape-recorder playback to increase bandwidth of chart recorder. Base line of current (i) and PDn traces indicate −80 mV level. Section 1 shows pulse timing (bar) in VD burst; sections 2–4 show expanded time-base records. *B*: isochronal current-voltage relation, measured at end of pulse. Points labeled 2, 3, and 4 correspond to records $A_{2,3,4}$. Filled circles, burst continued after pulse. Open triangles, burst was terminated; note that terminations commenced near the start of the lower linear region. m, slope; r, correlation coefficient for lines, which are least-square fits; n, number of points for lines. Ordinate: absolute membrane potential (*G40*).

to the onset of normal bursts in PD driver cells (Fig. 4*B*), in the LP follower cell (Fig. 6*A*, trace 1), and in other follower cells. The concave-upward accelerating trajectory is suggestive of voltage-dependent regenerative activation, being the inverse of the trajectories in Fig. 11*A, B, D*. The dissimilar behavior of a passive cable model and the absence of phasic synaptic input during the burst onset phase in the follower neurons (cf. Fig. 3) have already been noted.

This "accelerating trajectory" behavior was associated with nonlinear current-voltage relations. As above, a graded series of hyperpolarizing pulses was given at a fixed point during burst depolarizations (see Fig. 12*A* for an example for a VD cell). An isochronal plot of the voltage level reached by the end of the pulse (Fig. 12*B*) showed two linear regions with a transition zone between. The upper linear regions suggest a high conductance during the burst, confirmed by the relatively short time constant of the membrane potential trajectory (Fig. 12A_2; see also Fig. 11*A*, −4.8-nA trace). The lower region suggests a lower conductance at more negative potentials, consistent with the voltage-dependent turning off of a conductance. (As before, a brief 32-ms pulse was used to avoid overlap with synaptic input arriving at later phase and was too short to allow the voltage response in Fig. 12A_4 to reach steady state; therefore, the input resistance of the rest state was underestimated.) The records in Fig. 11*A* and *D* would give corresponding nonlinear *I-V* relations for the LP and PD cells. The data indicate that a voltage-dependent increase in conductance occurs during the prolonged depolarization.

Endogenous burst termination

Phasic inhibition from other network cells undoubtedly plays an important role in the normal termination of follower-cell bursts, and for that reason we have instead mainly analyzed the burst-onset and prolonged depolarization phases. However, there were signs that the follower cells possess endogenous mechanisms for repolarization (burst termination) and pacemaking.

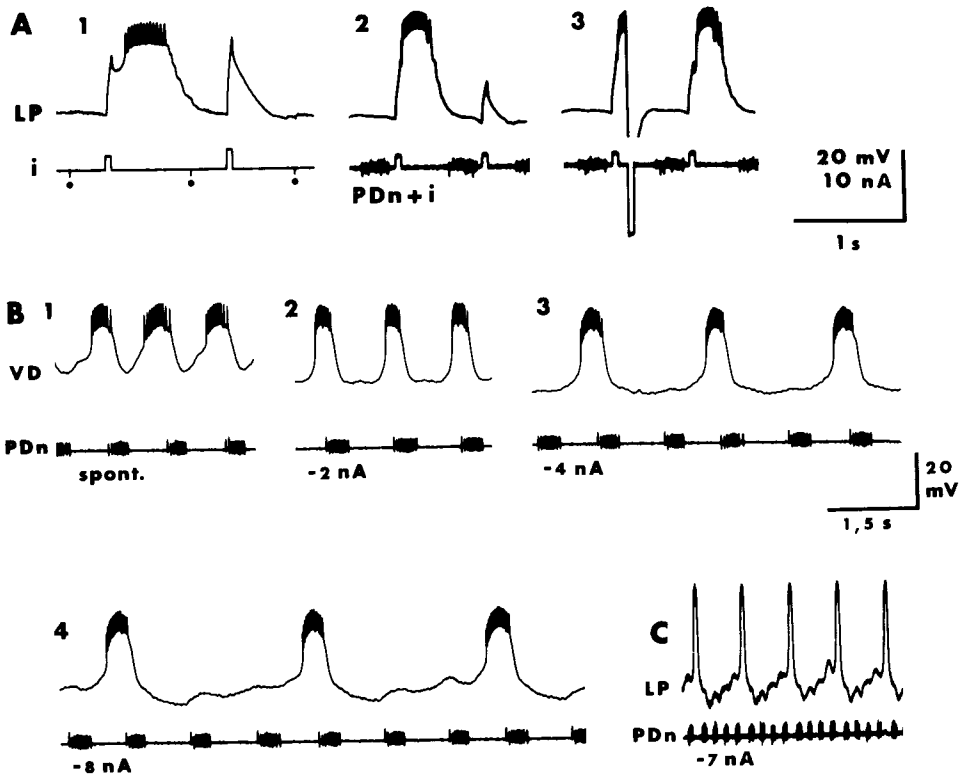

FIG. 13. *A*: double-pulse experiments to show LP refractoriness after triggered bursts. Slow modulation was eliminated by blocking the commissural and esophageal ganglia with 0 Ca^{2+} -2 × Mg^{2+} saline; pyloric P inputs were eliminated. Section 1: offset, −2.5 nA; circles indicate start of driver bursts. Sections 2, 3: offset , −6 nA; lower trace shows both PD bursts and bath current monitor (*G84*). *B*, *C*: offset currents modulated the burst rate in follower cells. The commissural and esophageal ganglia were blocked with 0.1 × Ca^{2+} -6 × Mg^{2+} saline to make the excitability constant. *B*: VD cell, with offsets indicated. Base line of PDn trace indicates a fixed V_m level for sections 1–4, but the absolute V_m was not known. Double-barrel electrode (*G57*). *C*: LP cell from same preparation, at slower time base, with regular escape bursts.

REFRACTORINESS. A period of reduced excitability followed a burst, as shown by double-pulse tests of triggering a burst and then subsequently attempting to trigger another burst (see Fig. 4*H* for the driver group, and Fig. 13*A* for the LP cell). Depending on the delay, the second current pulse could fail to trigger another burst even though its current intensity was higher, the rest V_m level was normal, and a larger stimulus depolarization was produced (Fig. $13A_1$). The latter suggests an elevated voltage threshold for triggering bursts. The degree of refractoriness depended on the duration of a burst, since if it were prematurely terminated, then another burst could be triggered just afterward (Fig. $13A_2$ and A_3); the action potential in frog node of Ranvier behaves similarly (45). Another contributor to refractoriness was a prolonged hyperpolarization following a burst, visible in Fig. $5B_2$ and 13*C*. Refractoriness might contribute to autotermination of bursts and might help determine the timing of repetitive bursts.

BURST-RATE MODULATION. Depolarizing current injected into the PD driver cells acted to increase their burst rate, while hyperpolarizing current slowed the burst rate in a manner smoothly graded with current intensity, as in other free-run endogenous oscillators (2, 8, 9, 21, 50–52). Hyperpolarizing current also modulated the burst rate in the pyloric follower neurons except that the rate modulation was not smoothly graded with current intensity. Instead, follower-cell bursts were entrained in integer multiples of the cycle period set by the driver group due to the strong driver → follower synaptic input.

For example, Fig. 13*B* shows a VD follower cell which, when increasingly hyperpolarized, produced bursts in ratios of 1:1, 1:2, 1:3, etc., with respect to the driver-group bursts (PDn trace). In this preparation, the central ganglia were blocked with low-Ca^{2+} saline to stop the operation of other slower pattern generators (METHODS) so that "slow modulation" of excitability was eliminated and was not the cause of the long-term VD and LP (Fig. 13*C*) periodicity. Note in section 2 that despite a −2-nA offset, the VD cell was still entrained 1:1 to the driver group with little change in cycle period compared to section 1 (even though the VD bursts had changed in waveform and shifted to later phase in section 2). Also, a depolarizing offset could not increase the burst rate of follower neurons beyond that of the driver group (under normal conditions). We have observed this burst rate modulation for the VD and LP neurons and related behavior in PE neurons. It suggests that the follower cells have endogenous tendencies for repetitive bursting.

BURST RESET. Free-run endogenous bursters can have their cycle timing reset by an intracellular current pulse, as in Fig. 4*C* and *D* for the driver group (15). Even though the follower neurons are strongly entrained, we looked for signs of burst reset in hyperpolarized cells undergoing regular "escape" bursts (as in Fig. 13*C*). From limited data on LP neurons, it appears that prematurely triggering a burst with a current pulse under such conditions can reset the subsequent rhythm of escape bursts.

Other pyloric follower neurons

Each neuron type in the pyloric system has its own distinctive characteristics, and they differ enough to warrant demonstration of regenerative properties for each. We found that each type has a regenerative capability. The basic data for triggering and repolarization and the exclusion of network explanations are emphasized here.

VD NEURON. The relevant synaptic connections to VD are indicated in Fig. 14*A*; in par-

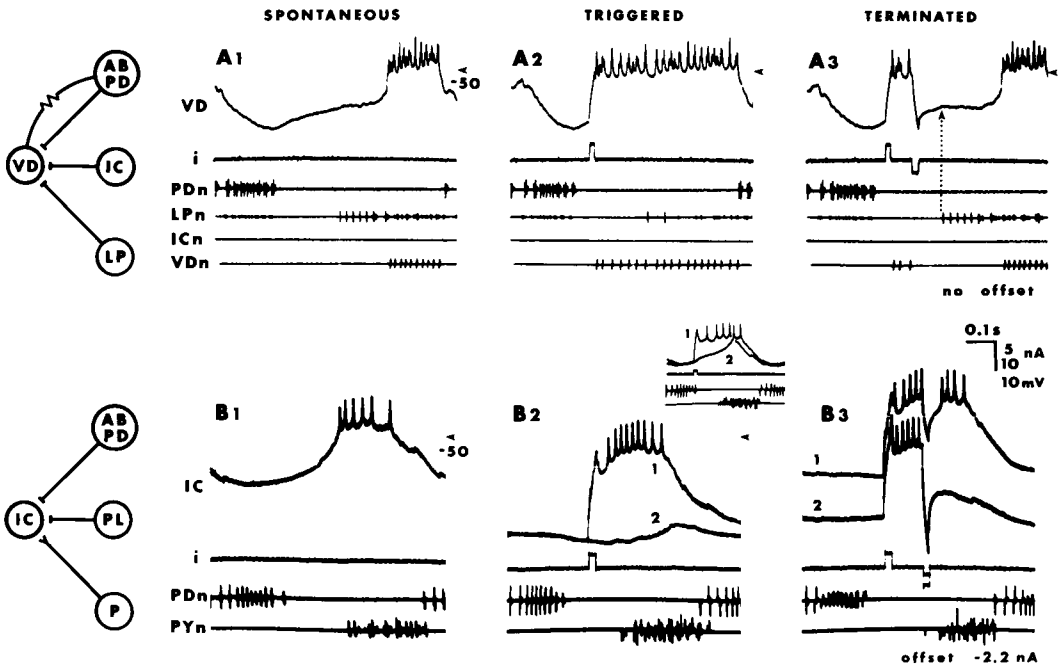

FIG. 14. *A*: VD neuron, no offset thoughout. The pyloric P inputs were eliminated. ICn (showing no firing of the IC cell) and VDn were separately monitored by splitting the median ventricular nerve—see Table 1 (*G46*). *B*: IC neuron. No offset in B_1 and inset; hyperpolarized by −2.2 nA in B_2 and B_3. Inset and B_2: cycle 2 immediately preceded cycle 1. B_3: cycles 1 and 2 were taken at same phase of the gastric rhythm. PYn shows firing of both PL and PE types (*G43*). All horizontal arrows, −50 mV. See Fig. 2 for circuit-diagram conventions. Current calibration is 5 nA (*A*) and 10 nA (*B*). Calibrations for inset are proportional.

ticular, the LP → VD inhibition is significant. The VD neuron consistently showed powerful burst depolarizations. These could readily be triggered and terminated in the nonpolarized cell (no offset), indicating that the plateau mechanism does operate within and contribute to normal oscillations. Spectacular shifts in the timing of onset of VD bursts could be produced by premature triggering (no offset), more so than for any other pyloric follower cell type. In Fig. 14A_2, a depolarizing pulse was given at a time when all the presynaptic neurons were silent, so the "triggered" premature start of VD firing could not be attributed to disinhibition. As before, we have also made such triggering when the presynaptic LP neuron was impaled and strongly hyperpolarized to prevent its inhibiting VD, another way of excluding network explanations. In the "terminated" example (Fig. 14A_3), a VD plateau was triggered by a depolarizing pulse and then soon afterward terminated by a hyperpolarizing pulse, such that the VD membrane potential remained repolarized for about 80 ms before the start of LP firing (correcting for LP propagation time); repolarization was not attributable to synaptic inhibition for this time at least (which was as long as 150 ms in other examples). Note that the voltage transient during the termination pulse did not exceed the normal trough V_m level, indicating that the threshold for repolarization was indeed within the normal operating range. Strong plateaus can also be triggered in hyperpolarized VD cells (41; see Fig. 9*B*).

IC NEURON. The primary inputs to IC are inhibition by the PD-AB driver neurons and also the PL follower neurons (the IC neuron is like "another LP neuron"). Bursting activity of IC varied from nil to intense in different preparations. Note the prominent, smooth, concave-upward, accelerating trajectory leading to the onset of spontaneous bursts in Fig. 14B_1. Bursts could be triggered by brief depolarizing pulses, prematurely in nonpolarized cells (inset, Fig. 14B_2) and in all-or-none fashion in hyperpolarized cells (Fig. 14B_2). A threshold for repolarization is illustrated in Fig. 14B_3 for the hyperpolarized IC cell. Variation in spike timing of presynaptic cells was within the normal range and did not appear to explain this behavior of IC.

PL NEURONS. There are several synaptic inputs to a PL cell, but it is mainly the driver group that needs to be considered, since the other inputs are relatively weak (17). The large spontaneous oscillations could be suppressed by a weak (−0.7 nA) hyperpolarizing pulse straddling the expected burst phase (revealing some P-cell EPSPs; Fig. 15A_1): we take this as evidence that voltage-dependent plateau properties normally contribute to PL oscillations. PL neurons showed nonlinear *I-V* behavior to a series of hyperpolarizing pulse given at constant phase during bursts (as in Fig. 12); the discontinuity appeared at V_m levels wthin the normal operating range (not illustrated). Regenerative behavior is demonstrated in a hyperpolarized PL cell in Fig. 15A_2 and A_3. Neither triggering nor termination of PL bursts could be attributed to changes in timing of the driver group. Tests on this PL cell did not appear to affect bursting of another PL-cell, monitored extracellularly (large unit, PLn trace), suggesting that the electrical coupling among PLs had a minor role, if any, in the behavior observed.

Despite the large oscillations in membrane potential (up to 25 mV spontaneously), we had difficulty demonstrating adequate triggering or repolarization in a PL neuron without the aid of hyperpolarizing offsets.

PE NEURONS. The main input to PE neurons is inhibition from the driver group, making it simple to exclude network explanations for regenerative behavior. PE neurons often underwent marked slow modulation of burst activity, although bursting tended to be weak, with about 10-mV oscillations in membrane potential. Even so, when hyperpolarized they were almost unique in consistently producing regenerative responses lasting for two cycles of the pyloric rhythm (provided that impalement damage was minimal). A brief depolarizing pulse elicited a prolonged depolarization (Fig. 15B_2), which continued through the next driver-group burst, although PE firing did stop during this driver-group burst. A two-cycle response could be terminated at any point (Fig. 15B_3); the threshold current for repolarization was lowest for hyperpolarizing pulses given during the intervening driver-group burst. It was difficult to demonstrate triggering or repolarization in PE neurons without the use of

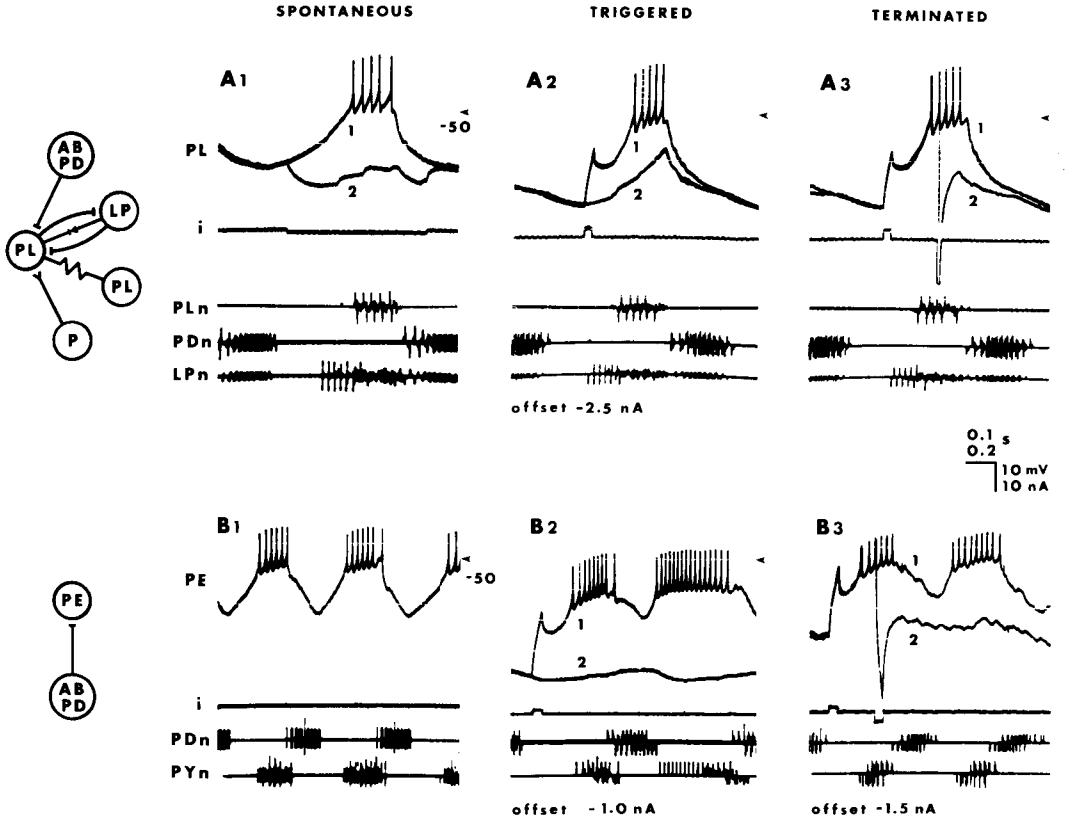

FIG. 15. *A*: PL neuron. No offset in A_1, trace 1; hyperpolarized by −2.5 nA in A_2 and A_3. A_1: cycle 1 immediately preceded cycle 2. A_2: cycle 2 immediately preceded cycle 1. A_3: sweeps 1 and 2 were taken at same phase of esophagus rhythm (*G44*). *B*: PE neuron. B_1: no offset. B_2: same cell as B_1, but now with pyloric P inputs eliminated; control sweep 2 was somewhat before test sweep 1 (*G45*). B_3: another PE cell, showing tonic EPSPs; sweeps 1 and 2 were made at similar phase of slow modulation (*G58*). All horizontal arrows, −50 mV. See Fig. 2 for circuit-diagram conventions. Lower time calibration applies to *B*.

hyperpolarizing offsets, perhaps on account of their typically weak spontaneous activity.

DISCUSSION

We conclude that all neurons in the pyloric generator, including all the follower neurons as well as the driver neurons, have an endogenous membrane capability for generating prolonged regenerative depolarizations. These can be termed regenerative plateau potentials, as in other systems such as cardiac muscle. Plateaus are accompanied by a voltage-dependent increase in conductance. Our indirect tests indicate that a sustained negative-resistance characteristic, due to a slow inward-current mechanism activated by a depolarization, most likely underlies the regenerative plateaus. Lines of evidence summarized below indicate that regenerative plateaus are the primary driving force for axonal spiking during bursts in all the follower and driver neurons and largely determine the timing of burst onset in many follower neurons. Plateau potentials in the pyloric-system neuron appear to share many characteristics with prolonged regenerative potentials in numerous other systems such as vertebrate cardiac muscle (28, 53), vertebrate smooth muscle (34), endogenously bursting neurons in crustacean cadiac ganglion (48, 52) and mollusks (2, 12, 29), certain neurons for the leech heart rhythm (5), cat motoneurons (43), frog node of Ranvier (45), and axons treated with special drugs or ionic solutions (1, 46).

Tests for regenerative capability

One approach would be to voltage clamp the follower cells, directly demonstrate a neg-

ative-resistance characteristic in each cell type, and measure its activation threshold and time course, etc. However, the pyloric generator is like many other rhythmically active networks in that *1*) the component neurons are tightly coupled into a synaptic network, and *2*) access to the active regions of STG neurons is restricted due to problems of the neuronal geometry, making accurate voltage-clamp analysis difficult. In such nonideal situations, there is general need for criteria and experimental approaches for deciding whether a given neuron's oscillating membrane potential and bursting firing pattern are due to regenerative cellular properties, or to synaptic connections, or both (2, 5, 8–10, 23, 30, 34, 41, 44, 56).

Characteristic electrical behaviors of cells with regenerative plateau mechanisms include the following (see references above): *1*) Bistable behavior: bursts can be triggered or terminated by current pulses; two preferred levels of membrane potential are observed with rapid transitions in between. *2*) Threshold: a certain current intensity is required to trigger or terminate bursts; metastable behavior and inflections are other signs of thresholds. *3*) Stimulus independence: responses act all or none, since their amplitude and waveform tend to be independent of stimulus strength, once suprathreshold. *4*) Regenerative feedback behavior: responses grow after a near-threshold stimulus and outlast passive responses in symmetrical pulse tests; accelerating trajectories indicate progressive activation or deactivation. *5*) Voltage dependency: this is indicated by sigmoidal (nonlinear) *I-V* curves, threshold behavior, burst suppression by hyperpolarizing offset currents, and symmetrical pulse tests. *6*) Repetitive recurrence: cells with regenerative plateau mechanism often also have mechanisms for self-termination of bursts and pacemaking, giving rise to repetitive endogenous bursting, refractoriness, burst-rate modulation by offset currents, and burst reset by brief stimuli.

Alternative mechanisms

NETWORK EXPLANATIONS. We have studied spontaneous activity in the normal ganglion, analogous to other larger systems in which one might like to study the in situ integration. The network-monitoring approach and stimulus-phase independence tests that we have used to exclude network explanations may be applicable in the analysis of rhythm generators in larger systems. If the individual PSPs in a system are typically small, intracellular stimuli to an individual neuron for plateau tests would presumably be incapable of significantly perturbing a pattern-generating network, so that a neuron would behave operationally as a follower even if it were part of the generator. It might then suffice to monitor the generator indirectly, e.g., by recording motoneuron bursts.

In the case of the pyloric generator, we knew in advance how many cells were involved in the network and their firing phase and waveform, and we could record the firing of all of them simultaneously. This aided the "network monitoring" approach. Some ambiguity can be recognized concerning the endogenous versus synaptic basis of repolarization behavior, since tests at late phase in a burst tended to overlap with subsequent inhibitory synaptic barrages. On the other hand, there is little reason to attribute the burst triggering, etc., to synaptic interactions, since the follower cells receive little or no synaptic input from the pyloric network during the silent period, the burst onset, and the duration of the burst (provided the P inputs were eliminated). This favorable situation for studying the prolonged burst depolarizations could be further improved by experimental means such as hyperpolarizing presynaptic cells during tests.

ALTERNATIVE CELLULAR MECHANISM. The criteria for slow regenerative behavior have been referenced to a negative-resistance-based mechanism, which is slowly or noninactivating. At present this appears to be the most likely explanation for plateau behavior in STG neurons. However, the criteria per se are consistent with other positive-feedback cellular mechanisms, which could give rise to, or contribute to, bistable behavior. For example, one view of the burst generation in hippocampal CA3 neurons, and in certain endogenously repetitive bursting neurons of mollusks, involves the summation of depolarizing spike afterpotentials (DAPs) as the source of or a contributor to the positive feedback producing the burst state (49, 55). Bursts in these cells can be triggered, terminated, etc. DAP mechanisms have been invoked to explain certain types of bursts in

other crustacean systems (52). However, we believe that DAPs make a minor contribution, if any, to bistability in pyloric-system neurons because *1*) spike generation is thought to be confined to the distal axon in crustacean motoneurons (this is why the spikes are highly attenuated in somatic recordings), *2*) the large-amplitude smooth-accelerating trajectories before the start of spiking in a burst (as Fig. 6*A*) would not be expected for a DAP mechanism (52), and *3*) neither would prolonged metastable behavior (as Fig. 8*B*). It is likely that the regenerative plateau mechanism is distinct from the spike mechanism and that plateaus depolarize the axon to drive repetitive spiking, as thought to be the case for other crustacean systems (47, 48, 52).

A possible explanation for the ability to terminate bursts with current pulses is that a hyperpolarizing pulse might enable (remove the inactivation from) a g_A mechanism, which then would prevent a cell from firing for a time. Such a voltage-dependent hyperpolarizing "delaying conductance" has been described in certain crustacean axons (6) and molluscan neurons. In the case of the LP neuron, it has been tested for delaying conductances, with largely negative results (16). However, the PL neurons have an effective delaying conductance, which may act to delay the onset of PL firing normally (16). The delaying conductance may explain some of the difficulty of triggering bursts in PL neurons.

Another interaction of cellular properties concerns axonal spiking, which can be expected to reset the membrane potential at the axon after each spike, and therefore may limit depolarization in other parts of a cell. This may affect the kinetics of slow regeneration activation and inactivation (compared to what they would be without axonal spiking) and therefore distort measurements of plateau time course and *I-V* relations.

Given the unipolar geometry of STG neurons (24), there is likely to be appreciable "electrical distance" between electrodes in a soma and the site of plateau generation, presumably dendritic. Voltage transients in a soma during current injection probably do not accurately reflect voltage levels at the site of plateau generation, more so when plateau currents are active. This will affect *I-V* relations and thresholds.

Cellular role of regenerative plateaus

OPERATING RANGE. One of our objectives was to establish that regenerative transitions occur within the range of membrane potential traversed by a cell's normal oscillations. It is conceivable that a cell's regenerative plateau mechanism might stay permanently on, with the membrane potential never dipping far enough negative to achieve regenerative repolarization. The cell would have regenerative capability but essentially remain in the upper state, being equivalent to a repetitively firing neuron.

Evidence that regenerative transitions in the LP, VD, and IC follower neurons as well as the PD driver neurons lie within the voltage range of normal oscillation includes the ability to trigger or terminate ongoing bursts (i.e., without using any offset current), observations of inflections, observations of accelerating trajectories, measurements of *I-V* relations, and measurements of triggering threshold V_m levels during metastable behavior. In these cells, it appears that the regenerative plateau mechanism is turning on and off with each oscillation.

Difficulties in triggering bursts in PL neurons have already been noted. Nevertheless, the suppression of bursts by weak hyperpolarizing currents (as Fig. $15A_1$), nonlinear *I-V* tests showing a discontinuity within the normal operating range, and the large amplitude of PL voltage excursions suggest that regenerative transitions occur with each cycle in these cells too.

We have observed endogenous bursting (below) and obtained positive tests for bistability in PE neurons, without using any offset current, when the level of activity was raised by stimulation of certain inputs (unpublished observations). However, PE neurons can exhibit a much wider range of behavior than their limited role in the pyloric synaptic circuit would indicate, e.g., long-period modulation of activity (concurrent with pyloric cycling), which appears to derive from intrinsic cell properties rather than synaptic input. A simple statement about PE bistability may be premature.

REGENERATIVE CONTRIBUTION TO BURST DEPOLARIZATIONS. Several lines of evidence indicate that the follower-neuron bursts would be weak or nonexistent without the

regenerative plateau mechanism. *1*) Most follower neurons stop firing and all show much smaller oscillations if the nerve connecting the STG centrally is cut or blocked (37, 39). This reduced pyloric activity was correlated with negative results in the various tests for plateau capability (41). Inversely, large oscillations and intense bursting activity (as here) were correlated with positive tests for regenerative plateaus. *2*) Hyperpolarization tests indicated that the major part of the burst oscillation in every type of follower neuron was voltage dependent (cf. Figs. 4, 5, 9*B*, 14B_2, 15A_1, 15B_2). In each case, hyperpolarization sharply reduced the amplitude of oscillations. Weak pulses straddling the normal burst time gave particularly effective demonstrations of voltage dependency (cf. Fig. 15A_1). *3*) With the P inputs eliminated, there is little or no phasic synaptic input to the follower neurons that could be driving their bursts. We conclude that the slow regenerative mechanism appears to be the major driving force for axon spiking during bursts in all the follower and driver neurons of the pyloric generator.

Plateaus and pattern generation

The possible role that bistable membrane properties might play in pattern production depends on how stable are the two states, rest and plateau, and how strong are the synaptic inputs to a given cell. At one extreme, a cell might tend to undergo spontaneous transitions between states, resulting in "one-shot" bursts or repetitive endogenous bursting. This seems to be the case with the driver cells, which receive only limited input from the network. Besides a regenerative plateau mechanism for driving bursts, they also appear to have strong endogenous mechanisms for repolarization (burst termination) and for pacemaking (controlling the cycle period). Cellular properties appear to dominate the behavior of the driver cells.

At the other extreme, a cell with a regenerative plateau mechanism might tend to be stable and undergo a state transition only when perturbed by a phasic synaptic input; EPSPs could trigger bursts and IPSPs could terminate bursts (41). Burst timing would be completely controlled by the phasic synaptic input, leaving the regenerative plateau properties to affect mainly the amplitude (intensity) of bursts.

ARE FOLLOWER NEURONS REPETITIVE ENDOGENOUS BURSTERS? There were signs that some or all of the follower neurons have endogenous mechanisms for repolarization and pacemaking and can undergo spontaneous state transitions, to some degree at least. If the driver group is hyperpolarized or for other reasons not active, the LP cell, or at least some neurons of the PL-PE group, can continue to burst repetitively, apparently bursting endogenously (3, 41; possible network interactions were monitored and shown to not be the source of the bursting). In addition, the progressive burst-rate decrease in LP and VD neurons with increasing hyperpolarizing offset (Fig. 13) has much of the character of endogenous repetitive bursting.

Within limits, the pyloric network might be viewed as a set of coupled oscillators, with synaptic connections as sources of entrainment. The driver group appears to have a faster cycle rate than the follower neurons (in the species studied here) and so would drive the system as the fastest oscillator. The analytical approaches of oscillator theory may be applicable (35).

TIMING OF BURST ONSET. Whether or not the followers can act as endogenous bursters, one can separately inquire as to the relative importance of intrinsic versus network factors in determining the timing of burst onset versus termination. The kinetics of regenerative plateau activation appear to make a major contribution to the timing of burst onset in the follower neurons (after being inhibited during the driver-group burst), an example of spontaneous transitions. For example, regenerative kinetics appear to dominate the burst onset in LP (in cases with P-cells eliminated), as evidenced by the lack of synaptic input at that phase of the pyloric cycle, by the accelerating trajectory observed, and by the ability of current pulses to advance or delay the burst onset. Additional factors affecting the burst onset in particular cells can include the decay of preceding synaptic inhibition, both impulse and nonimpulse mediated; excitation from P inputs; contributions from cellular properties such as rebound, rectification, delaying conductance, etc.; and *R-C* properties of the neuronal geometry.

TIMING OF BURST TERMINATION. In follower neurons, the end of bursts appears pre-

dominantly set by synaptic inhibition, an example of synapse-dominated behavior. For example, bursts in the LP and IC follower neurons terminate near the start of firing in the PL follower group, and the PL → LP and PL → IC inhibition is effective (17), with large IPSPs visible. Another example is that bursts in the VD follower neuron terminate near the start of driver-group firing, even when a VD plateau is triggered very prematurely (Fig. 14A_2; this implies that if the VD cell can self-terminate its bursts, the intrinsic burst length must be even longer). However, regenerative repolarization and intrinsic termination mechanisms (e.g., K^+ conductances) undoubtedly contribute to the membrane-potential trajectory seen during burst termination, in many or all of the follower neurons, as evidenced for example by endogenous bursting in the LP cell (41).

ACKNOWLEDGMENTS

Technical assistance by J. Fok, D. Gassie, S. McCarthy, and C. Sirchia, manuscript preparation by C. Kosaki, and manuscript comments by M. Miller are gratefully acknowledged.

This study was supported by National Institutes of Health Grants NS 13138 and NS 15314.

Address requests for reprints to D. F. Russell, Békésy Laboratory of Neurobiology.

Received 12 August 1980; accepted in final form 11 May 1982.

Assistance by M. Bidaut and P. Lenz is also gratefully acknowledged.

REFERENCES

1. ADELMAN, W. J., JR. Electrical studies of internally perfused squid axons. In: *Biophysics and Physiology of Excitable Membranes*, edited by W. J. Adelman, Jr. New York: Van Nostrand, 1971, p. 274–319.
2. ARVANITAKI, A. AND CHALAZONITIS, N. Electrical properties and temporal organization in oscillatory neurons. In: *Neurobiology of Invertebrates*, edited by J. Salanki. New York: Plenum, 1968, p. 169–199.
3. BIDAUT, M. *Dissection pharmacologique du réseau pylorique dans le ganglion stomatogastrique chez la Langouste* (These de troisième cycle). Bordeaux, France: Université de Bordeaux II, 1980.
4. BIDAUT, M. Pharmacological dissection of pyloric network of the lobster stomatogastric ganglion using picrotoxin. *J. Neurophysiol.* 44: 1089–1101, 1980.
5. CALABRESE, R. L. The roles of endogenous membrane properties and synaptic interaction in generating the heartbeat rhythm of the leech, *Hirudo medicinalis*. *J. Exp. Biol.* 82: 163–176, 1979.
6. CONNOR, J. A. Neural repetitive firing: a comparative study of membrane properties of crustacean walking leg axons. *J. Neurophysiol.* 38: 922–932, 1975.
7. FRIESEN, W. O. AND STENT, G. S. Neural circuits for generating rhythmic movements. *Ann. Rev. Biophys. Bioeng.* 7: 37–61, 1978.
8. GÄHWILER, B. H. AND DREIFUSS, J. J. Phasically firing neurons in long-term cultures of the rat hypothalamic supraoptic area: pacemaker and follower cells. *Brain Res.* 177: 95–103, 1979.
9. GAINER, H. Electrophysiological behavior of an endogenously active neurosecretory cell. *Brain Res.* 39: 403–418, 1972.
10. GILLARY, H. L. AND KENNEDY, D. Pattern generation in a crustacean motoneuron. *J. Neurophysiol.* 32: 595–606, 1969.
11. GOLA, M. Neurones à ondes-salves des mollusques. Variations cycliques des conductances ioniques. *Pfluegers Arch.* 352: 17–36, 1974.
12. GOLA, M. Electrical properties of bursting pacemaker neurons. In: *Neurobiology of Invertebrates: Gastropoda Brain*, edited by J. Salanki. Budapest: Akademiai Kiado, 1976, p. 381–424.
13. GOLDMAN, Y. AND MORAD, M. Regenerative repolarization of the frog ventricular action potential: a time and voltage-dependent phenomenon. *J. Physiol. London* 268: 575–611, 1977.
14. GRAUBARD, K., RAPER, J., AND HARTLINE, D. K. Nonspiking synaptic transmission between spiking neurons. *Soc. Neurosci. Abstr.* 3: 177, 1977.
15. HARTLINE, D. K. Quantitative analysis of pyloric network in stomatogastric ganglion. *Soc. Neurosci. Abstr.* 2: 324, 1976.
16. HARTLINE, D. K. Pattern generation in the lobster (*Panulirus*) stomatogastric ganglion. II. Pyloric network simulation. *Biol. Cybern.* 33: 223–236, 1979.
17. HARTLINE, D. K. AND GASSIE, D. V., JR. Pattern generation in the lobster (*Panulirus*) stomatogastric ganglion I. Pyloric neuron kinetics and synaptic interactions. *Biol. Cybern.* 33: 209–222, 1979.
18. HARTLINE, D. K., GASSIE, D. V., AND SIRCHIA, C. D. Additions to the physiology of the stomatogastric ganglion (STG) of the spiny lobster, *Panulirus interruptus*. *Soc. Neurosci. Abstr.* 5: 248, 1979.
19. HARTLINE, D. K. AND MAYNARD, D. M. Motor patterns in the stomatogastric ganglion of the lobster *Panulirus argus*. *J. Exp. Biol.* 62: 405–420, 1975.
20. HODGKIN, A. L. The subthreshold potentials in a crustacean nerve fibre. *Proc. R. Soc. London Ser. B* 126: 87–121, 1938.
21. HODGKIN, A. L. The local electric changes associated with repetitive action in a non-medullated axon. *J. Physiol. London* 107: 165–181, 1948.
22. HODGKIN, A. L., HUXLEY, A. F., AND KATZ, B. Measurement of current-voltage relations in the membrane of the giant axon of *Loligo*. *J. Physiol. London* 116: 424–448, 1952.
23. KATER, S. B. AND KANEKO, C. R. S. An endogenously bursting neuron in the gastropod mollusc, *Helisoma trivolis*. *J. Comp. Physiol.* 79: 1–14, 1972.
24. KING, D. G. Organization of crustacean neuropil. II. Distribution of synaptic contacts on identified motor neurons in lobster stomatogastric ganglion. *J. Neurocytol.* 5: 239–266, 1976.
25. MAYNARD, D. M. Simpler networks. *Ann. NY Acad. Sci.* 193: 59–72, 1972.

26. MAYNARD, D. M. AND DANDO, M. R. The structure of the stomatogastric neuromuscular system in *Callinectes sapidus, Homarus americanus* and *Panulirus argus* (Decapoda Crustacea). *Philos. Trans. R. Soc. London Ser. B* 268: 161–220, 1974.
27. MAYNARD, D. M. AND SELVERSTON, A. I. Organization of the stomatogastric ganglion of the spiny lobster. IV. The pyloric system. *J. Comp. Physiol.* 100: 161–182, 1975.
28. MCALLISTER, R. E., NOBLE, D., AND TSIEN, R. W. Reconstruction of the electrical activity of cardiac Purkinje fibres. *J. Physiol. London* 251: 1–59, 1975.
29. MEECH, R. W. Membrane potential oscillations in molluscan "burster" neurones. *J. Exp. Biol.* 81: 93–112, 1979.
30. MOFFETT, S. Neuronal events underlying rhythmic behaviors in invertebrates. *Comp. Biochem. Physiol. A* 57: 187–195, 1977.
31. MOULINS, M. AND VEDEL, J.-P. Programmation centrale de l'activité motrice rythmique du tube digestif antérieur chez les Crustacés décapodes. *J. Physiol. Paris* 73: 471–510, 1977.
32. MULLONEY, B. Organization of the stomatogastric ganglion of the spiny lobster. V. Coordination of the gastric and pyloric systems. *J. Comp. Physiol.* 122: 227–240, 1977.
33. NOBLE, D. Applications of Hodgkin-Huxley equations to excitable tissues. *Physiol. Rev.* 46: 1–50, 1966.
34. OHBA, M., SAKAMOTO, Y., AND TOMITA, T. The slow wave in the circular muscle of the guinea-pig stomach. *J. Physiol. London* 253: 505–516, 1975.
35. PAVLIDIS, T. *Biological Oscillators: Their Mathematical Analysis.* New York: Academic, 1973.
36. RUSSELL, D. F. Phasic inputs to the lobster stomatogastric ganglion. *Soc. Neurosci. Abstr.* 1: 594, 1975.
37. RUSSELL, D. F. *Central Control of Pattern Generators in the Stomatogastric Ganglion of the Lobster Panulirus interruptus.* (Ph.D. Dissertation). La Jolla: Biology Dept. University of California, 1977.
38. RUSSELL, D. F. P cells: distribution and coupling of pattern generators in the lobster stomatogastric nervous system. *Soc. Neurosci. Abstr.* 4: 384, 1978.
39. RUSSELL, D. F. CNS control of pattern generators in the lobster stomatogastric ganglion. *Brain Res.* 177: 598–602, 1979.
40. RUSSELL, D. F. AND HARTLINE, D. K. Inputs to the lobster stomatogastric ganglion unmask bursting properties in many of its motorneurons. *Soc. Neurosci. Abstr.* 3: 385, 1977.
41. RUSSELL, D. F. AND HARTLINE, D. K. Bursting neural networks: a reexamination. *Science* 200: 453–456, 1978.
42. RUSSELL, D. F. AND HARTLINE, D. K. A multiaction synapse evoking both EPSPs and enhancement of endogenous bursting. *Brain Res.* 223: 19–38, 1981.
43. SCHWINDT, P. AND CRILL, W. E. A persistent negative resistance in cat lumbar motoneurons. *Brain Res.* 120: 173–178, 1977.
44. STRUMWASSER, F. Types of information stored in single neurons. In: *Invertebrate Nervous Systems. Their Significance for Mammalian Neurophysiology*, edited by C. A. G. Wiersma. Chicago: University of Chicago Press, 1967, p. 291–319.
45. TASAKI, I. Initiation and abolition of the action potential of a single node of Ranvier. *J. Gen. Physiol.* 39: 377–395, 1956.
46. TASAKI, I. AND HAGIWARA, S. Demonstration of two stable potential states in the squid giant axon under tetraethyl-ammonium chloride. *J. Gen. Physiol.* 40: 859–885, 1957.
47. TAZAKI, K. AND COOKE, I. M. Spontaneous electrical activity and interaction of large and small cells in cardiac ganglion of the crab, *Portunus sanguinolentus. J. Neurophysiol.* 42: 975–999, 1979.
48. TAZAKI, K. AND COOKE, I. Isolation and characterization of slow, depolarizing responses of cardiac ganglion neurons in the crab, *Portunus sanguinolentus. J. Neurophysiol.* 42: 1000–1021, 1979.
49. THOMPSON, S. H. AND SMITH, S. J. Depolarizing afterpotentials and burst production in molluscan pacemaker neurons. *J. Neurophysiol.* 39: 153–161, 1976.
50. TRAUTWEIN, W. AND KASSEBAUM, D. G. On the mechanism of spontaneous impulse generation in the pacemaker of the heart. *J. Gen. Physiol.* 45: 317–330, 1961.
51. WALL, P. D. Repetitive discharge of neurons. *J. Neurophysiol.* 22: 305–320, 1959.
52. WATANABE, A., OBARA, S., AND AKIYAMA, T. Pacemaker potentials for the periodic burst discharge in the heart ganglion of a stomatopod, *Squilla oratoria. J. Gen. Physiol.* 50: 839–862, 1967.
53. WEIDMANN, S. Effect of current flow on the membrane potential of cardiac muscle. *J. Physiol London* 115: 227–236, 1951.
54. WILSON, W. A. AND WACHTEL, H. Negative resistance characteristic essential for the maintenance of slow oscillations in bursting neurons. *Science* 186: 932–934, 1974.
55. WONG, R. K. S. AND PRINCE, D. A. Participation of calcium spikes during intrinsic burst firing in hippocampal neurons. *Brain Res.* 159: 385–390, 1978.
56. WYMAN, R. J. Neural generation of the breathing rhythm. *Ann. Rev. Physiol.* 39: 417–448, 1977.